Gondwana Research 21 (2012) 406–421

Contents lists available at ScienceDirect

Gondwana Research

journal homepage: www.elsevier.com/locate/gr

Assembly of Pampia to the SW Gondwana margin: A case of strike-slip docking?

Cecilia M. Spagnuolo [a,*], Augusto E. Rapalini [b], Ricardo A. Astini [c]

[a] CONICET-IESGLO, Instituto de Sedimentología, Facultad de Ciencias Naturales y Fundación Miguel Lillo, Universidad Nacional de Tucumán, Miguel Lillo 251, T4000JFE, San Miguel de Tucumán, Argentina
[b] CONICET-INGEODAV, Depto. Cs. Geológicas, FCEyN, Univ. Buenos Aires, Pabellón 2, Ciudad Universitaria, C1428EHA, Buenos Aires, Argentina
[c] Laboratorio de Análisis de Cuencas, CICTERRA, CONICET-Universidad Nacional de Córdoba, Avenida Vélez Sársfield 1611, X5016GCA Córdoba, Argentina

ARTICLE INFO

Article history:
Received 12 November 2010
Received in revised form 2 February 2011
Accepted 3 February 2011
Available online 12 February 2011

Keywords:
Paleomagnetism
Northwestern Argentina
Gondwana
Paleozoic
Pampia

ABSTRACT

Different hypotheses have been proposed to account for the geologic evolution of the southwestern margin of Gondwana in the Early Paleozoic, involving accretion and displacement of different terranes in a protracted convergent margin. In order to constrain and understand the kinematic and paleogeographic evolution of the Pampia terrane a paleomagnetic study was carried out in different Cambrian to Devonian units of the Eastern Cordillera (Cordillera Oriental) and the Interandean Zone (Interandino) of NW Argentina. Paleomagnetic poles from the Campanario Formation (Middle to Upper Cambrian): 1.5°N 1.9°E $A_{95}=9.2°$ $K=37.46$ $N=8$; and Santa Rosita Formation (Lower Ordovician): 8.6°N 355.3°E $A_{95}=10.1°$ $K=26.78$ $n=9$, representative of the Pampia terrane, are interpreted to indicate a Late Cambrian significant displacement with respect to the Río de la Plata and other Gondwana cratons. A model, compatible with several geological evidences that explains this displacement in the framework of the final stages of Gondwana assembly is presented. We propose a simple dextral strike-slip kinematic model in which Pampia and Antofalla (−Arequipa?) blocks moved during Late Cambrian times from a position at the present southern border of the Kalahari craton into its final position next to the Rio de la Plata craton by the Early Ordovician.

1. Introduction

It is well known nowadays that the final assembly of Gondwana was achieved after a series of multiple collisions (e.g. Meert et al., 2001, 2003; Sánchez Bettucci and Rapalini, 2002; Kroner and Cordani, 2003; Tohver et al., 2006; Trindade et al., 2006) in the Late Neoproterozoic and Early Paleozoic during the Brasiliano (600–550 Ma) and Pampean (550–510 Ma) orogenic cycles (Ramos, 1999; Collo et al., 2009; Hauser et al., 2011). According to Meert (2001) and Meert et al. (2001) the main orogenic events ended around 530–500 Ma, although movements of small blocks may have continued afterwards. However, the configuration, history and paleogeography during the Gondwana amalgamation is quite debatable because of the scarcity of reliable paleomagnetic data (Cordani et al., 2000; Sánchez Bettucci and Rapalini, 2002; Meert and Torsvik, 2003; Tohver et al., 2006; Cordani et al., 2009).

Spagnuolo et al. (2008) carried out a paleomagnetic survey on the Middle–Late Cambrian Mesón Group, exposed in the province of Salta, NW Argentina (22°49′–22°50′S; 64°50′–65°00′W). The results of this study permitted to obtain the first Cambrian paleomagnetic pole (FC) for NW Argentina, which suggests that the area underwent a significant clockwise rotation. Three alternatives were proposed in that work: i) FC pole is representative of Gondwana and implies a complex APWP with high drift velocities of the supercontinent; ii) significant displacement of Pampia during the final stages of Gondwana assembly; iii) an Andean rotation related to the regional deflections associated to the Bolivian Orocline. Considering that the original paleomagnetic data came from a single locality and no age for the rotation was available, Spagnuolo et al. (2008) chose the more conservative third alternative as the most likely.

The aim of this work is to provide new paleomagnetic data in order to test the original interpretation of Spagnuolo et al. (2008) and to better constrain the paleogeographic evolution of the Pampia Terrane (Fig. 1) in the Early Paleozoic, when the final processes of Gondwana assembly were taking place. Pampia (see Ramos et al., 2010 for a review) is located to the west of the Río de la Plata craton (Rapela et al., 2007; Favetto et al., 2008), to the east of the Cuyania composite terrane (Villar, 1975; Kraemer et al., 1995; Escayola et al., 1996; Ramos, 2000) and to the north of the North-Patagonian Massif (Chernicoff and Zappettini, 2003). Its northern boundary is not precisely defined due to the thick cover of Cenozoic sediments of the Chaco-Pampean plains. The oldest exposed rocks of the Pampia block are Late Neoproterozoic units of different metamorphic grade, with generally higher grades towards the south in the Córdoba and San Luis Ranges (e.g. Sims et al., 1998; Steenken et al., 2004; Fig. 1) and lower grades in the metasediments of the Puncoviscana Formation in the Eastern Cordillera (Aceñolaza and Toselli, 1981; Rapela et al., 1998a, b; Fig. 1).

* Corresponding author.
E-mail addresses: cecispagnuolo@yahoo.com.ar (C.M. Spagnuolo), rapalini@gl.fcen.uba.ar (A.E. Rapalini), raastini@gtwing.efn.uncor.edu (R.A. Astini).

1342-937X/$ – see front matter
doi:10.1016/j.gr.2011.02.004

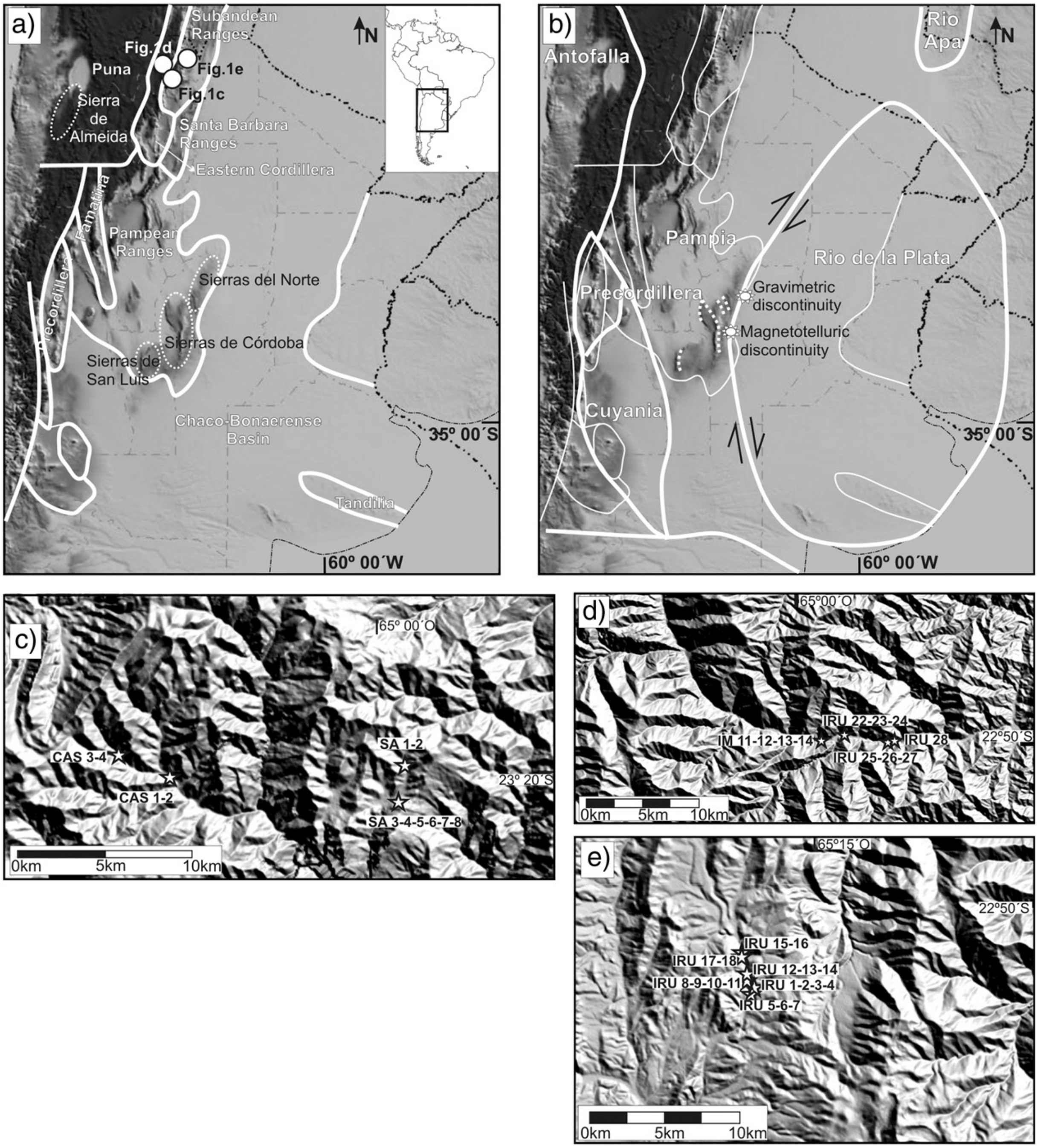

Fig. 1. a) North and central Argentina with the sampling areas and the morphotectonic provinces. b) Terrane boundaries (Astini, 2003; Ramos, 2004; Rapela et al., 2007; Favetto et al., 2008; Tohver et al., 2008; Ramé and Miró, 2010) and shear zones (dotted lines) of Martino (2003), Simpson et al. (2003). c) Digital elevation model of Caspalá–Santa Ana locality and the paleomagnetic samples (white stars). CAS 1–2: Santa Rosita Formation, CAS 3–4: Baritú Formation. d) Digital elevation model of Matancillas locality and the paleomagnetic samples and sites (white stars). IM 11–14: Campanario Formation (Spagnuolo et al., 2008), IRU 25–28: Lizoite Formation, IRU 22–24: Santa Rosita Formation. e) Digital elevation model of Parada del Condor locality and the paleomagnetic samples (white stars). IRU 1–7: Lizoite Formation. IRU 8–18: Campanario Formation.

Several tectonic models support the accretion of a parauthochthonous or fully allochthonous Pampia Terrane (Ramos, 1988; Kraemer et al., 1995; Escayola et al., 1996; Rapela et al., 1998a, b, 2001; Von Gosen et al., 2002; Ramos et al., 2010) to the Río de la Plata craton. They either propose eastward (present coordinates) subduction of oceanic crust under the Rio de la Plata craton (Kraemer et al., 1995; Escayola et al., 1996; Escayola et al., 2007) or subduction to the west, under Pampia (Ramos, 1988). The age of this collision is also under discussion, some authors suggesting the Neoproterozoic (Ramos, 1988; Kraemer et al., 1995; Escayola et al., 2007) and others the Early–Middle Cambrian (Rapela et al., 1998b; Von Gosen et al., 2002; Steenken et al., 2004; Ramos, 2008; Ramos et al., 2010). Different regions or cratons have been proposed for the origin of this terrane. Rapela (2000) and Von Gosen et al. (2002) postulated that Pampia originated close to the Río de la Plata craton. Links with the Arequipa–Antofalla terrane have also been proposed (Rapela et al., 1998b; Keppie and Bahlburg, 1999; Bahlburg et al., 2000; Rapela, 2000; Kleine et al., 2004; Collo et al., 2009) as well as with Amazonia (Tosdal, 1996; Sims et al., 1998; Sánchez Bettucci and Rapalini, 2002; Steenken et al., 2004; Rapela et al., 2007; Adams et al., 2008a; Ramos et al., 2010) and the Kalahari craton (Schwartz and Gromet, 2004; Whitmeyer and Simpson, 2003; Rapela et al., 2007; Drobe et al., 2009).

Non collisional tectonic models suggest that after deposition of the Puncoviscana Formation (and equivalent units to the south), on a passive margin developed on the Río de la Plata craton (Piñán Llamas and Simpson, 2006), eastward subduction began on that margin and finished with the collision of an oceanic spreading ridge at around 525 Ma (Miró et al., 2005; Piñán Llamas and Simpson, 2006; Schwartz et al., 2008).

Paleomagnetism is the only tool to quantitatively define the displacement and geographic positions of terranes in pre-Jurassic times. In order to constrain the paleogeographic position of Pampia and its relations with other West Gondwana cratons in Cambrian times, new paleomagnetic studies were carried out on Cambrian, Ordovician and Devonian sedimentary units in NW Argentina.

2. Geological setting

The Central Andes in northwestern Argentina (Gansser, 1973; Ramos, 1999) are presently affected by normal subduction (~30°) of the Nazca Plate under South America. This region is subdivided, from west to east, into the Puna, Eastern Cordillera (Cordillera Oriental) and Subandean Ranges (Sierras Subandinas) morphotectonic provinces (Fig. 1a). The regional structures of the Eastern Cordillera constitute a dominant thick-skinned, east-vergent thrust system (Keidel, 1943). Its eastern margin, which includes its transitional boundary with the Subandean Ranges, is known as the Interandean Zone (Kley, 1996), and is characterized by double vergence structures (Baldis et al., 1976) and a high topographic relief.

The stratigraphy of this region consists of metasediments assigned to the Ediacaran–Early Cambrian Puncoviscana Formation (Turner, 1960; Buatois and Mángano, 2003; Schwartz and Gromet, 2004; Do Campo and Ribeiro Guevara, 2005; Adams et al., 2008a); Middle to Late Cambrian shallow platform quartzites, sandstones and red to greenish shales of the Mesón Group (Turner, 1960); Ordovician marine successions of sandstones interbedded with conglomerates and black shales best represented by the Santa Victoria Group (Turner, 1960; Astini, 2003); marine clastic sediments with iron beds of Silurian–Devonian age (Astini, 2003); fluvial and eolian deposits of Carboniferous–Permian age; sediments and volcanics of the Cretaceous–Lower Paleocene Salta Group rift basin and Cenozoic sediments of the Andean foreland basin (Mon and Salfity, 1995).

The Middle to Late Cambrian Mesón Group is subdivided into three units: the Lizoite, Campanario and Chahualmayoc Formations. The Campanario Formation is a dominantly green and purple fine-grained, thoroughly bioturbated succession with minor fine-grained sandstones (Mángano and Buatois, 2004). Its age is bracketed between the Middle and Late Cambrian according to stratigraphic considerations (Turner, 1960; Sánchez and Salfity, 1999; Aceñolaza and Aceñolaza, 2002; Astini, 2008) and between Early and Middle Cambrian according to ichnofossils (Mángano and Buatois, 2004). Adams et al. (2008b) and Augustsson et al. (submitted for publication) have recently obtained a maximum depositional age by SHRIMP and LA-ICP-MS U–Pb on detrital zircons in the range of 521–502 Ma, suggesting Late Cambrian as the most likely age for this unit.

The Santa Rosita Formation, which is the basal unit of the Ordovician Santa Victoria Group, is composed of Late Cambrian to Late Tremadocian (Buatois and Mángano, 2003) sandy and shaly shallow marine packages interbedded with some conglomerates (Astini, 2003).

The Baritú Formation is characterized by sandstones and white and purple silty shales assigned to the Late Silurian–Early Devonian (Turner and Méndez, 1975; Dalenz-Farjat et al., 2002).

3. Paleomagnetic sampling and methods

In the field, oriented hand-sample blocks were collected. At the laboratory each block was drilled in order to obtain 4 to 7 cylindrical cores, which were sliced into one to three standard paleomagnetic specimens (2.2 cm height and 2.54 cm diameter).

The Lizoite quartz-rich sandstones (with no positive paleomagnetic results) and Campanario Formation were sampled at Parada del Cóndor locality (22.9°S 65.3°W; Fig. 1e) in the eastern part of the Santa Victoria Ranges. Eleven samples (4 sites) were collected from the Campanario Formation obtaining 43 specimens (see Table 1).

The Santa Rosita Formation was sampled at three localities: Matancillas (22.8°S 64.9°W; Fig. 1d), Santa Ana (23.3°S 65.0°W; Fig. 1c) and Caspalá (23.3°S 65.1°W; Fig. 1c). At Matancillas three hand samples (1 site) were drilled obtaining 21 specimens, at Santa Ana 8 hand samples (2 sites) were drilled in 29 specimens and at Caspalá 13 specimens were obtained from 2 hand samples (1 site) (see Table 1).

A preliminary paleomagnetic study of the Baritú Formation was carried out in Caspalá (23.3°S 65.1°W; Fig. 1c). Two hand samples from 1 site were collected (9 specimens, Table 1)

Intensity and direction of the natural remanent magnetization were measured with a DC-SQUID (2G-750R) cryogenic magnetometer. AF cleaning was achieved by means of a static three-axes degausser attached to the cryogenic magnetometer. Thermal demagnetization was applied with an ASC dual chamber oven, with internal magnetic fields below 5 nT. Bulk magnetic susceptibility was

Table 1
Samples collected at each locality.

Unit	Site	Sample	Specimen						
Locality: Parada del Cóndor									
Campanario Formation	PC 1	IRU 8	A-a	A-b	B				
		IRU 9	A	B-b	B-c				
		IRU 10	B	C	D	E			
		IRU 11	A	B	C				
	PC 2	IRU 12	A	B	C	D	E	F	
		IRU 13	A	B	C	D	E	F	
		IRU 14	A	B	C-a	C-b	E	F	
	PC 3	IRU 15	A	B	C				
		IRU 16	C						
	PC 4	IRU 17	A	B-a	B-b	C	D	E	F
		IRU 18	B						
Formación Lizoite	PC5	IRU 1	B	C	D	E	F		
		IRU 2	A	B	C-a	C-b	D	E	
		IRU 3	A	B	C				
		IRU 4							
	PC 6	IRU 5	A	B	C	D			
		IRU 6	A-a	A-b	B	C	D	E	F
			G						
		IRU 7	A	B	C				
Locality: Matancillas									
Lizoite Formation	MAT 1	IRU 25	A	B	C				
		IRU 26	A	B	C				
		IRU 27	A	B	C	D			
	MAT 2	IRU 28	A-b	A-c	B	C	D	E	
Santa Rosita Formation	MAT 3	IRU 22	A	B	C	D	E	F	
		IRU 23	A	B	C	D	E	G	
		IRU 24	A	B	C	D	E	G	H-b
			H-a	I					
Locality: Santa Ana									
Santa Rosita Formation	STA 1	SA 1	A-a	A-b	B	C	D		
		SA 2							
	STA 2	SA 3							
		SA 4	A	B	C-a	C-b	D		
		SA 5	A	B-b	B-c	C			
		SA 6	A	B	C				
		SA 7	A	B	C-a	C-b	D	E	
		SA 8	A	B	C	D	E	F	
Locality: Caspalá									
Santa Rosita Formation	CA 1	CAS 1	C	D	E	F	G	H	L
			M	N					
		CAS 2	A	B	C				
Baritú Formation	CA 2	CAS 3	A	B-a	B-b	C	D		
		CAS 4	A	B	C	D			

Table 2
Susceptibility axes (k1, k2, and k3). Int: Intensity, D: declination. I: inclination (both in geographic coordinates). *: after structural correction. L: lineation. F: foliation. P: anisotropy degree. T: shape parameter. a) Campanario Formation. N = 6: without IRU11 site. b) Santa Rosita Formation.

Specimen	k1					k2					k3					L	F	P	T
	Int	D	I	D*	I*	Int	D19	I	D*	I*	Int	D	I	D*	I*				
a) Campanario Formation																			
IRU 9A	1.0211	340	27	156	3	1.0173	239	19	246	5	0.9616	119	55	45	84	1.004	1.058	1.062	0.876
IRU 10B	1.0177	326	32	143	1	1.0132	59	1	55	12	0.9690	149	58	238	79	1.004	1.046	1.050	0.820
IRU 11A	1.0122	157	9	135	38	1.0006	50	59	1	50	0.9872	252	29	261	8	1.012	1.014	1.025	0.082
IRU 11B	1.0065	11	12	189	5	0.9990	103	9	95	39	0.9945	230	75	285	51	1.008	1.005	1.012	−0.247
IRU 12B	1.0135	341	27	341	0	1.0113	249	2	250	4	0.9753	155	63	69	86	1.002	1.037	1.039	0.888
IRU 13D	1.0142	65	9	62	4	1.0130	331	26	152	1	0.9728	172	63	257	86	1.001	1.041	1.042	0.945
IRU 14B	1.0129	277	9	98	3	1.0041	13	33	8	9	0.9830	173	55	200	81	1.009	1.021	1.030	0.417
IRU 15A	1.0198	342	32	342	1	1.0109	251	13	72	8	0.9693	142	55	245	82	1.009	1.043	1.052	0.656
N = 8	1.0130	356	27	162	1	1.0080	252	7	72	3	0.9800	149	62	275	87	1.005	1.028	1.033	0.695
N = 6	1.0150	329	30	322	0	1.0120	239	1	52	2	0.9730	147	60	231	88	1.003	1.039	1.043	0.835
b) Santa Rosita Formation																			
SA 4B	1.0272	1	24	356	2	1.0134	143	61	229	87	0.9594	264	16	87	3	1.014	1.056	1.071	0.604
SA 5B-b	1.0294	5	29	358	8	1.0181	157	58	220	79	0.9525	268	12	89	8	1.011	1.069	1.081	0.716
SA 5B-c	1.0289	5	30	358	9	1.0173	163	59	230	77	0.9538	269	9	89	11	1.011	1.066	1.079	0.700
SA 7D	1.0292	356	21	173	2	0.9992	135	63	329	88	0.9716	260	16	83	1	1.030	1.028	1.059	−0.027
SA 7E	1.0275	358	22	174	0	1.0066	142	64	276	86	0.9659	263	14	85	4	1.021	1.042	1.064	0.336
SA 8A	1.0306	19	29	9	13	1.0149	145	47	161	75	0.9545	271	29	277	7	1.015	1.063	1.080	0.600
N = 6	1.0280	4	23	359	2	1.0110	145	61	235	87	0.961	266	16	89	2	1.017	1.053	1.070	0.511

measured with a Bartington MS-2 susceptibility meter after each thermal step to control possible chemical changes induced by heating of the samples. Magnetic components were determined by principal component analysis (Kirschvink, 1980) with maximum angular deviation (MAD) values under 13° (only one remanence direction was determined with a MAD of 16.9°). Acquisition of isothermal remanent magnetization (IRM) curves was performed with a pulse magnetizer (ASC Scientific IM-10-30) in order to identify the magnetic carriers at each site. The anisotropy of magnetic susceptibility (AMS) was measured with a Kappabridge MFK 1-B at 15 different positions to define the AMS ellipsoid. All the laboratory analyses were carried out at the Paleomagnetic Laboratory (INGEO-DAV) of the Department of Geological Sciences of the Universidad de Buenos Aires (Argentina).

One pilot group of 6 specimens from the Campanario Formation in Parada del Cóndor locality was demagnetized with alternating fields (AF) in 16 steps: 3, 6, 9, 12, 15, 20, 25, 30, 35, 40, 50, 60, 70, 80, 90 and 100 mT. Another pilot group of 7 specimens was demagnetized with high temperatures in 19 steps: 100, 150, 195, 250, 300, 350, 400, 450, 480, 500, 520, 540, 560, 580, 600, 620, 640, 660 and 680 °C. According to the obtained results the remaining specimens of the collection were demagnetized by high temperatures in 11 steps: 190, 290, 400, 450, 500, 545, 580, 600, 640, 660 and 680 °C. Acquisition of IRM tests were performed by applying increasing direct magnetic fields in 14 steps of 17, 29, 44, 61, 90, 150, 250, 350, 450, 600, 1000, 1640 and 2400 mT, while back field were produced in 13 steps of 29, 61, 90, 122, 137, 150, 250, 302, 350, 400, 450, 600 and 735 mT. AMS studies were performed only in 8 specimens, as the Kappabridge MFK 1-B became available

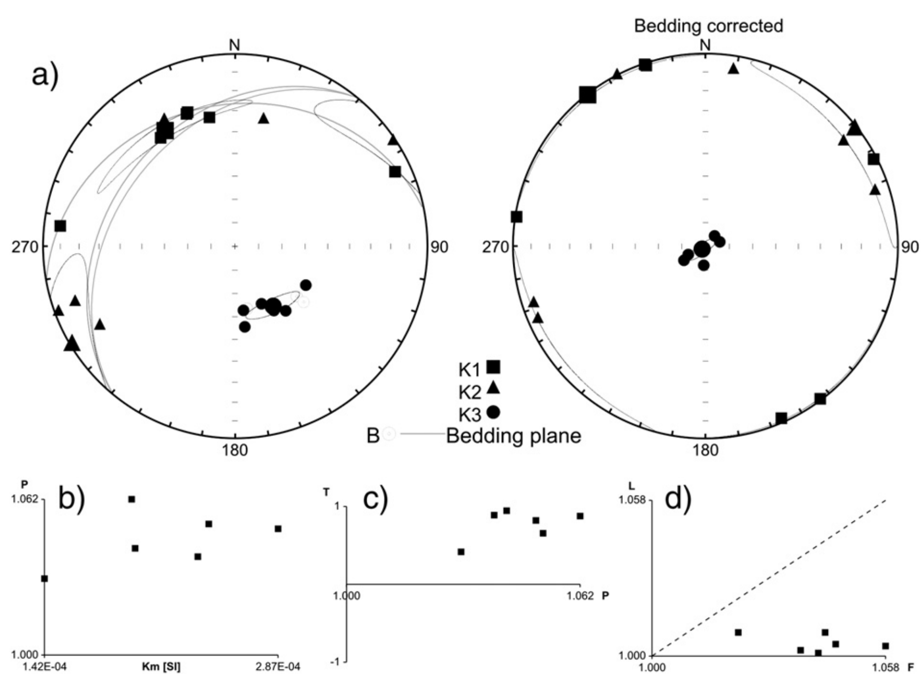

Fig. 2. Anisotropy of magnetic susceptibility of the Campanario Formation. a) *In situ* and bedding corrected distribution of the susceptibility axes. B: Bedding plane. b) Anisotropy degree (P) vs. average susceptibility (Km). c) Anisotropy degree (P) vs. shape parameter (T). d) Foliation vs. Lineation, Flinn's diagram (Jelinek, 1981).

after most of the collection had been already subjected to demagnetization.

The reported preliminary paleomagnetic study of the Santa Rosita Formation is the first one carried out in this Ordovician unit. AF demagnetizations were done in 17 steps between 3 and 100 mT and high temperature demagnetizations in 10 to 20 steps up to 680 °C.

4. Paleomagnetic results and interpretation

4.1. Campanario Formation

The AMS study shows an oblate fabric with a low degree of anisotropy, between 1.012 and 1.062 (Table 2a). After bedding correction, K3 coincides with the vertical while K1 and K2 are contained into the bedding plane (Fig. 2; Table 2a). These directional results plus the low anisotropy degree suggest a depositional or early diagenetic fabric.

Intensity of natural remanent magnetization varies between 0.287 and 30.85 mA/m and initial susceptibility between 3.9×10^{-5} and 18×10^{-5} (SI) indicating a wide variation between sites. Thermal demagnetization curves (Fig. 3) show that at Parada del Cóndor locality hematite is the main magnetic carrier with unblocking temperatures close to 680 °C, except for site IRU 11 that presented a much wider range of unblocking temperatures and from which no reliable directions were obtained. IRM curves (Fig. 4a) show saturation fields over 2500 mT, while the back field curves (Fig. 4a) show remanence coercivity of 550 mT, both suggesting that the dominant phase is hematite.

A high temperature magnetic component was isolated in most sites and samples except at IRU 11 (Fig. 3; Table 3). These paleomagnetic results are virtually identical to those (IM) obtained from the same formation at Matancillas (Spagnuolo et al., 2008; Fig. 1d), located ~35 km to the east from Parada del Cóndor (Fig. 1e). Remanence directions from both studies were merged and analyzed together. Comparison of mean site remanence directions before and after bedding correction indicates a significantly better grouping of directions after correction. This can be tested statistically by applying the fold test of Watson and Enkin (1993). After the application of the bedding correction the statistical parameters improve significantly: kappa (K) increases from 4.79 to 19.68 and α_{95} diminishes from 9.5° to 4.3° (Fig. 5). Since seven specimens showed opposite polarities, a reversal test was applied. The test of McFadden and McElhinny (1990) classified the result as positive, class "C" (critical angle: 16.2°, observed angle: 10.9°). Positive fold test and AMS results indicate a pre-tectonic magnetization. On the other hand, the occurrence of both

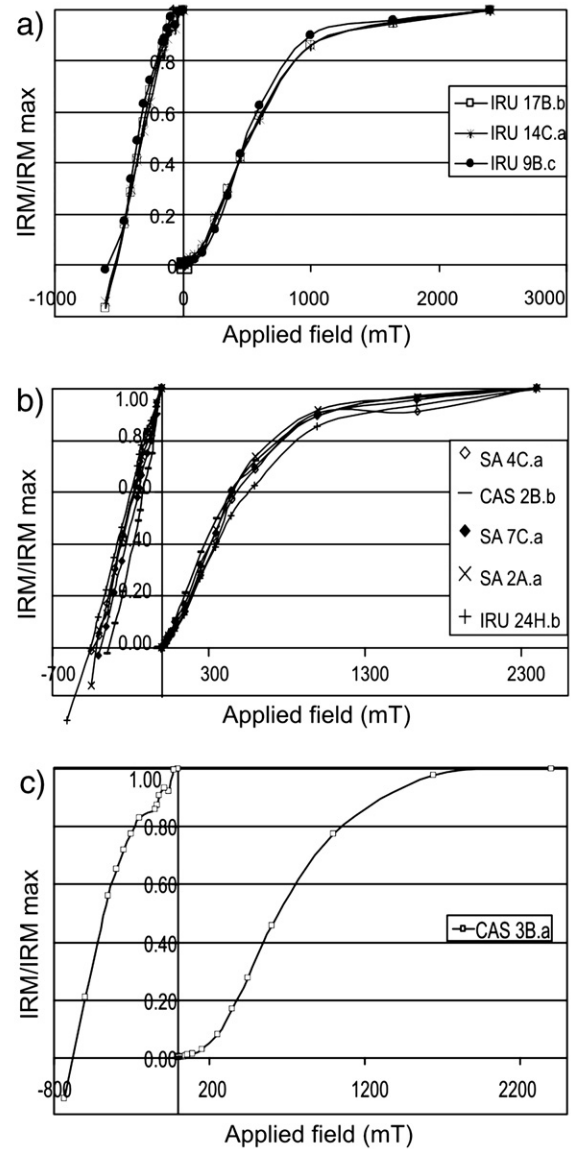

Fig. 4. Normalized isothermal remanent magnetization (IRM) curves. a) Campanario Formation specimens. The initial shallow slopes indicate hematite as the principal magnetic carrier. b) Santa Rosita Formation. c) Baritú Formation.

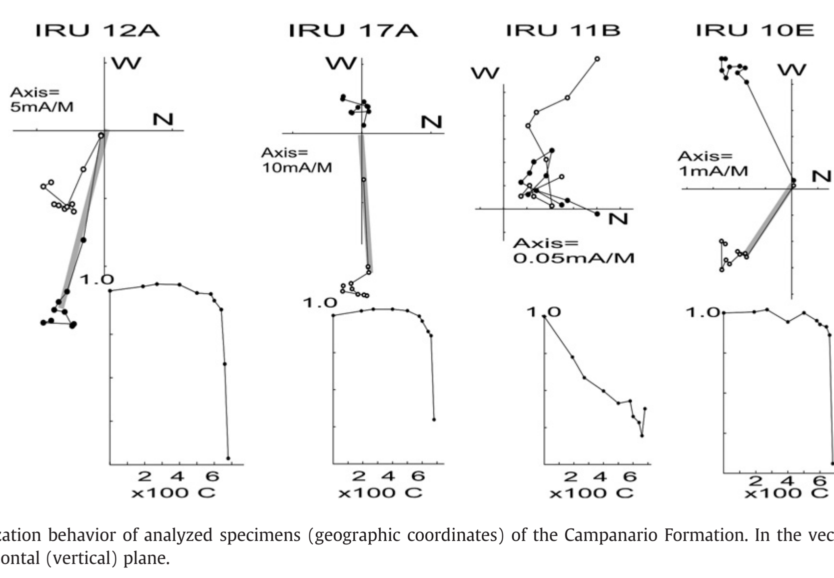

Fig. 3. Representative demagnetization behavior of analyzed specimens (geographic coordinates) of the Campanario Formation. In the vector diagram, closed (open) symbols represent projections on the horizontal (vertical) plane.

Table 3
Characteristic remanent magnetization of specimens, samples and sites of Campanario Formation. (*) Bedding corrected data. K and α_{95}: statistical parameters of Fisher (1953). Lat: latitude, (−) south latitude. Long: longitude. See Spagnuolo et al., 2008 for the detailed IM components.

Site/ sample	Specimen	D (°)	I (°)	MAD/α_{95} (°)	Bedding		D (°) (*)	I (°) (*)	VGP*	
					Strike (°)	Dip (°)			Lat	Long
Mean IM 11		123.0	79.9	9.7	K = 29.13	n = 9	94.5	44.6	−13.7	1.1
Mean IM 12		290.4	85.3	8.7	K = 35.68	n = 9	82.4	57.2	−8.7	356.0
Mean IM 13		85.1	60.0	–	K = −	n = 1	81.4	41.7	−1.8	359.6
Mean IM 14		67.6	54.4	5.2	K = 136.95	n = 7	68.8	23.4	14.1	4.8
IRU 8	8 A-b	284.0	−12.6	4.9	219	34	275.0	−42.5	13.3	183.4
	8 B	281.6	−3.5	3.3	219	34	275.8	−33.1	12.1	190.0
IRU 9	9 A	289.4	2.2	7.8	219	34	286.3	−29.7	20.8	195.6
	9 B-b	269.6	6.5	3.1	219	34	267.0	−19.6	1.2	194.2
IRU 10	10 B	249.6	14.4	5.4	219	34	252.3	−4.0	−15.4	195.7
	10 C	256.0	10.4	3.7	219	34	256.0	−10.5	−10.7	194.2
	10 E	245.9	28.2	4.4	219	34	256.1	9.7	−14.7	203.8
Mean PC 1		268.5	6.8	16.6	K = 14.13	n = 7	266.0	−19	1.0	193.8
IRU 12	12 A	103.8	22.6	4.0	253	27	90.4	33.9	−7.5	7.7
	12 B	105.4	22.4	4.9	253	27	92.1	34.4	−9.1	7.9
	12 C	113.2	22.7	3.1	253	27	99.9	37.9	−16.8	8.2
	12 D	104.8	20.6	3.5	253	27	92.5	32.5	−9.0	9.2
	12 E	105.9	14.3	3.7	253	27	96.8	27.3	−11.7	13.8
	12 F	96.2	23.8	1.7	253	27	82.4	31.6	0.1	6.0
IRU 13	13 A	100.3	36.4	2.9	253	27	77.9	44.2	0.2	356.3
	13 B	99.7	32.3	3.2	253	27	80.4	40.5	−0.7	359.8
	13 C	103.8	40.8	4.6	253	27	77.5	49.4	−1.4	352.2
	13 D	110.2	39.7	3.5	253	27	84.7	51.3	−7.7	353.2
	13 E	110.6	42.1	3.0	253	27	82.8	53.5	−7.0	350.6
	13 F	91.5	31.2	2.4	253	27	74.3	33.1	6.7	1.9
IRU 14	14 A	109.2	25.2	3.4	253	27	94.3	38.5	−12.0	6.0
	14 B	112.4	32.3	3.3	253	27	93.0	46.0	−12.8	0.1
	14 C-b	92.9	33.3	1.0	253	27	73.4	38.3	5.9	358.4
	14 E	101.4	24.0	0.7	253	27	87.3	34.1	−4.8	6.4
	14 F	100.9	26.1	3.4	253	27	85.5	35.7	−3.6	4.8
Mean PC 2		103.6	28.9	4.3	K = 70.12	n = 17	86.4	39.2	−5.4	2.5
IRU 15	15 A	73.0	16.6	3.1	219	38	56.2	33.7	21.3	352.5
	15 B	70.5	22.0	2.6	219	38	49.8	36.4	25.0	347.0
	15 C	74.9	6.3	4.0	219	38	64.9	26.4	16.6	1.2
Mean IRU 15		72.9	15.0	12.6	K = 96.52	n = 3	57.3	32.4	21.1	353.7
IRU 17	17 A	285.7	79.5	1.9	351	66	75.8	33.4	5.3	2.3
	17 B-a	330.1	77.5	2.1	351	66	67.8	27.9	13.7	1.8
	17 C	293.1	81.5	4.2	351	66	75.7	31.1	6.1	3.6
	17 D	321.9	81.5	4.5	351	66	72.6	27.9	9.6	4.0
	17 E	317.6	83.7	2.1	351	66	75.1	27.4	7.6	5.4
	17 F	271.5	78.5	4.7	351	66	78.4	35.3	2.6	2.3
Mean IRU 17		302.4	81.1	3.8	K = 310.93	n = 6	74.0	30.5	7.5	3.2
Specimens mean		Dec = 92.0° Inc = 53.9° α_{95} = 9.5° K = 4.79 R = 46.88 n = 59								
		Dec* = 81.5° Inc* = 37.7° α_{95}* = 4.3° K* = 19.68 R* = 56.05								
Mean VGP (samples): Lat: 1.5°S Long: 1.0°E A_{95} = 4.0° K = 22.90 n = 59										
Sites mean				Dec = 80.8° Inc = 69.5° α_{95} = 41.8° K = 2.71 R = 5.42 N = 8						
				Dec* = 78.3° Inc* = 36.5° α_{95}* = 10.8° K* = 27.45 R* = 7.74						
Mean VGP (sites): Lat: 1.5°N Long: 1.9°E A_{95} = 9.2° K = 37.46 N = 8										

polarities suggests that enough time elapsed during magnetization of the studied rocks to average out secular variation. A site-based mean of the bedding corrected remanence direction yields a direction at Dec = 78.3° Inc = 36.5° N (sites) = 8 α_{95} = 10.8° (Table 3 and Fig. 6). A virtual geomagnetic pole (VGP) was computed from each remanence direction. Their mean is the paleomagnetic pole calculated for the Campanario Formation (this result should replace the one published by Spagnuolo et al., 2008) FC2: 1.5°N, 1.9°E, A_{95} = 9.2°, K = 37.46, N = 8. The paleopole position indicates a paleolatitude of around 20° for deposition of the Campanario Formation sediments in the study region.

The recalculated paleomagnetic pole for the Campanario Formation is consistent with 6 of the 7 quality factor criteria of Van der Voo (1990), i.e.: i) the age of the rock is well known and different tests suggest a primary magnetization of the unit; ii) the result was obtained with enough number of samples and acceptable small errors; iii) samples were treated by standard demagnetization procedures and magnetic components calculated with principal component analyses (Kirschvink, 1980); iv) positive fold and v) reversal tests and vi) there is no matching of the paleopole with younger ones. All these arguments suggest that the FC2 paleopole is a reliable recording of the Late Cambrian magnetic field at the Eastern Cordillera.

When rotating the pole into African coordinates, according to the Euler pole 43.017°N 329.935°E 58.842° (Reeves et al., 2004) the position of the paleomagnetic pole became 33.7°N 34.7°E (Fig. 7). The comparison of this pole with different paleomagnetic poles of Gondwana (Grunow and Encarnación, 2000; Meert et al., 2001; McElhinny et al., 2003) show a significant clockwise rotation (Fig. 7).

4.2. Santa Rosita Formation

The samples from the Matancillas (Table 1) locality show IRM acquisition curves that do not saturate until 2 T (Fig. 4b; IRU 24) and back field curves (Fig. 4b; IRU 24) that show a remanence coercivity of 450 mT, characteristic of hematite. Demagnetization curves show unblocking temperatures of 580 °C (magnetite) and ~640 °C (Ti-hematite) (Fig. 8a). At higher temperatures the samples showed

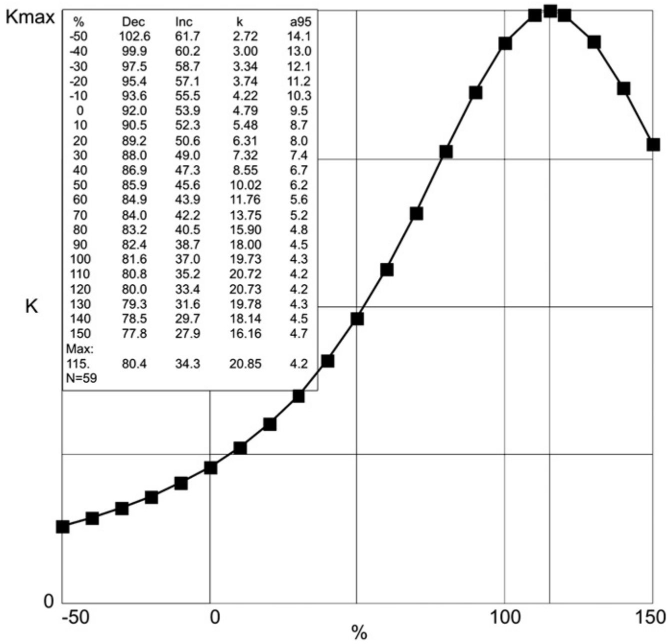

Fig. 5. Fold test of Watson and Enkin (1993) of the Campanario Formation.

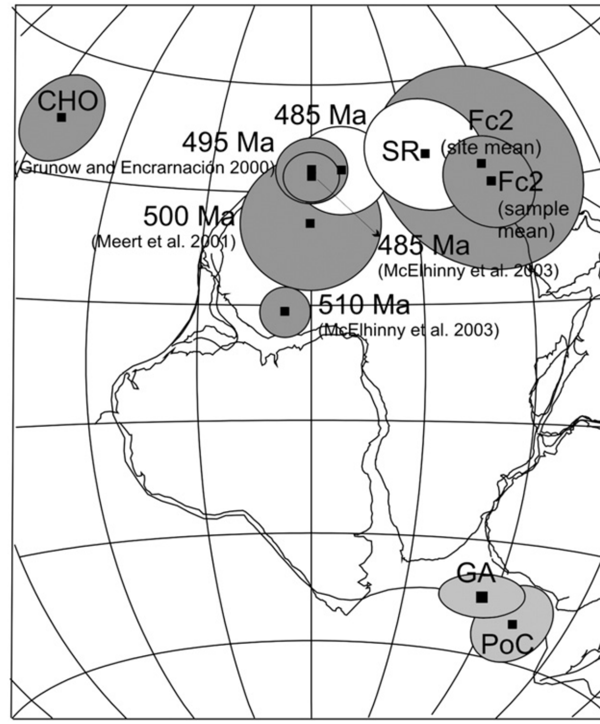

Fig. 7. Paleomagnetic poles from Lower Paleozoic NW Argentina and N Chile and the 485 (Grunow, 1995), 485 (McElhinny et al., 2003), 495 (Grunow and Encarnación, 2000), 500 (Meert et al., 2001) and 510 Ma (McElhinny et al., 2003) mean poles of Gondwana. CHO: Choschas Granite (Forsythe et al., 1993), SR: Santa Rosita Formation (this work), Fc2: Campanario Formation (this work), GA: Achala Granite (Geuna et al., 2008) and PoC: Baritú Formation (this work). South America poles were rotated to Gondwana configuration according to the Euler rotation pole 43.017°N 329.935°E 58.842° (Reeves et al., 2004) Africa in its present position.

viscous behaviors. Two components were isolated from these samples (Fig. 8a): a low-temperature (A) and an intermediate-temperature (between 200 °C and 580 °C) carried by magnetite (B). Component A was randomly oriented, while component B was the only one present in most of the samples with a good directional consistency.

IRM curves for samples from Caspalá locality indicate the presence of hematite and a ferrimagnetic phase (Fig. 4b; CAS 2). The demagnetization curves (Fig. 8b) show unblocking temperatures of 680 °C (hematite). A component of low temperature (A) was defined between 0 °C and 500 °C (associated to the ferrimagnetic phase), while a component of higher temperature (B) was isolated between 510 °C and 680 °C (Fig. 8b). Component A has a random distribution while component B is well grouped.

Samples of site STA 2 from Santa Ana locality have initial susceptibilities between 40×10^{-5} and 317×10^{-5} SI and NRM intensities between 0.419 and 566.700 mA/m. There is a direct correlation between higher initial magnetization intensity and susceptibility values with coarser grain sizes. IRM and back field curves (Fig. 4b; SA 4) indicate the presence of hematite and magnetite. Demagnetization curves present unblocking temperatures of 680 °C (hematite) and 580 °C (magnetite). Two components were defined (Fig. 8c): a low-temperature (A) between 175 °C and 580 °C in three specimens associated to magnetite and a high-temperature

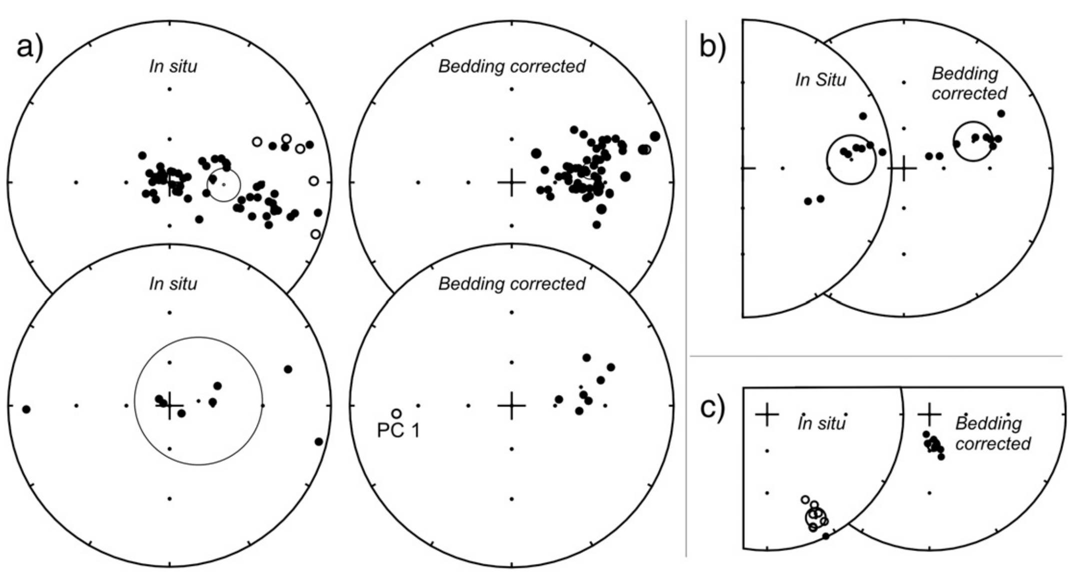

Fig. 6. *In situ* and bedding corrected distribution of specimen remanence directions of the analyzed formations. Equal-angle stereoplot, open (closed) symbol corresponds to negative (positive) inclination. a) Campanario Formation, in the bottom diagrams is the distribution of sites. b) Santa Rosita Formation. c) Baritú Formation.

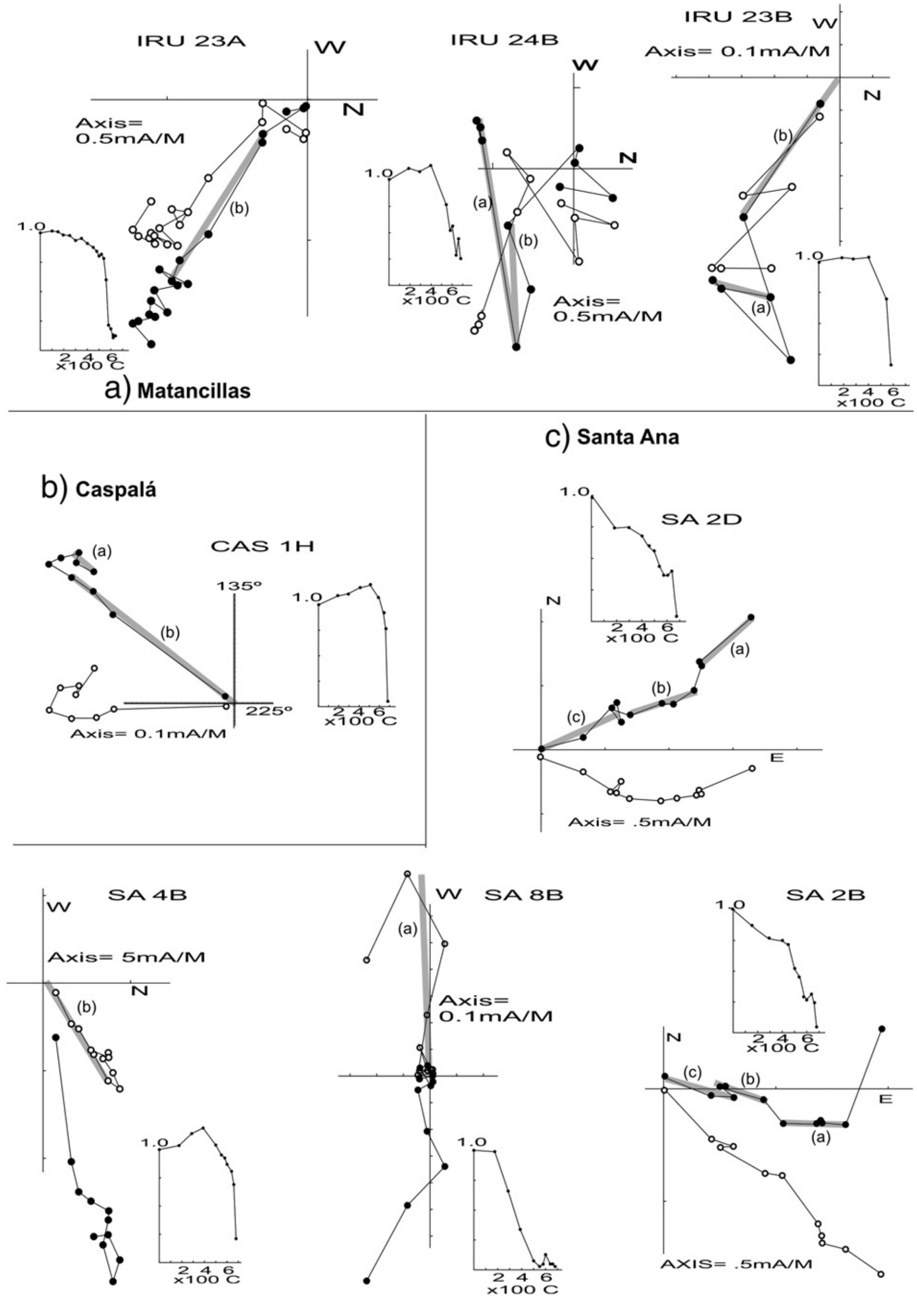

Fig. 8. Representative demagnetization behavior of analyzed specimens (geographic coordinates) of the Santa Rosita Formation. In the vector diagram, closed (open) symbols represent projections on the horizontal (vertical) plane.

(B) up to 680 °C that reaches the origin of coordinates and was used to calculate a VGP. AMS studies (Table 2b) indicate an anisotropy degree of 7% and an oblate magnetic fabric, which is interpreted of tectonic origin since K3 (minimum susceptibility axis) is horizontal (Fig. 9). This suggests some caution in interpreting the paleomagnetic data from this locality as the magnetic remanence might be affected by tectonic deformation. Since no systematic directional IRM studies could be performed, this issue is not defined.

IRM curves (Fig. 4b; SA 2) for site STA 1 from Santa Ana locality show the presence of both hematite and magnetite. Demagnetization curves (Fig. 8c) have unblocking temperatures of 580 °C (magnetite) and 680 °C (hematite) with soft slopes suggesting a wide grain size variation. Three components were obtained: a low-temperature (A), an intermediate one (B) carried by magnetite and a high-temperature (C) associated with hematite. The magnetite and hematite phases carry components of the same direction. VGP's were calculated from component B, since this is the most representative and is present in most samples.

At each site one VGP (Table 4) was obtained from each block sample by considering an average of characteristic remanence directions. Mean directions show a better clustering after bedding correction suggesting a pre-tectonic remanence. The elongated distribution of the directions (Fig. 6b) suggests that some directions from these localities may be suffering from some inclination error, as no significant changes are observed in declination, but only in inclination.

In situ mean direction is $D = 85.6°$ $I = 17.6°$ $\alpha_{95} = 12.1°$ $K = 18.98$ $N = 9$ (samples). After bedding correction, a slightly better grouping is observed: $D = 68.9°$ $I = 37.0°$ $\alpha_{95} = 12.0°$ $K = 19.34$ (Table 4 and Fig. 6b), although the fold test of Watson and Enkin (1993) and the tilt test of Enkin (2003) yield undetermined results. The calculated paleomagnetic pole for the Santa Rosita Formation,

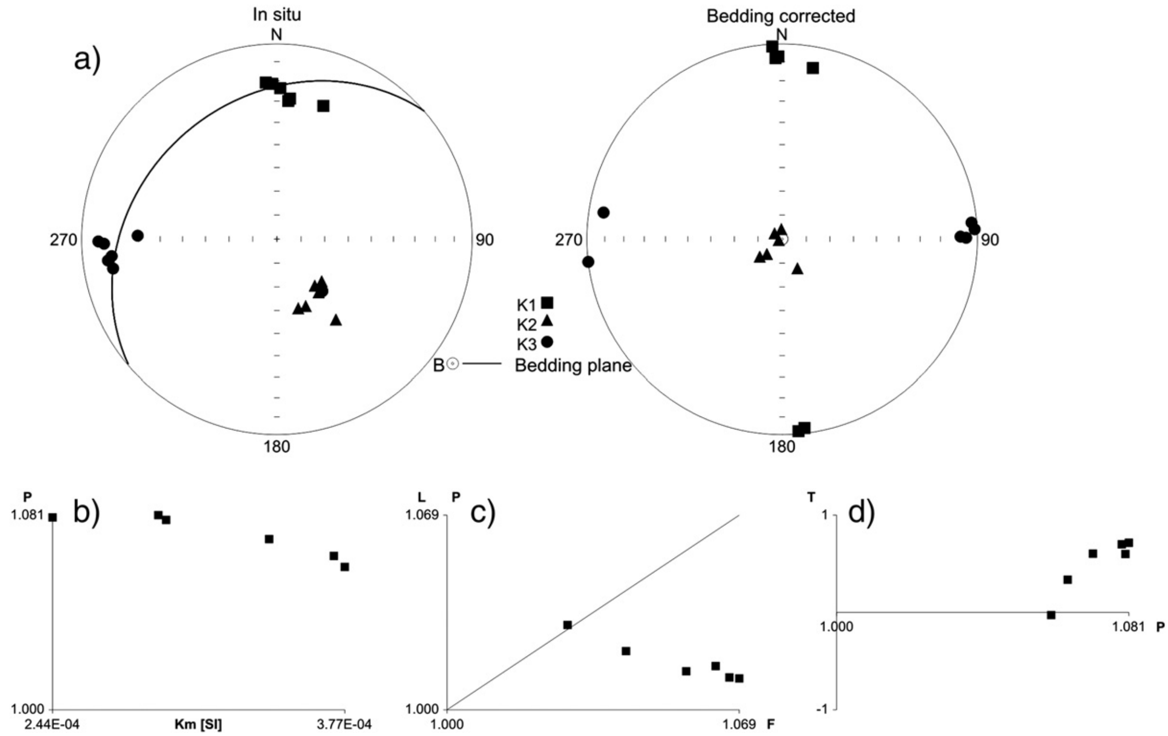

Fig. 9. Anisotropy of magnetic susceptibility of the Santa Rosita Formation. a) *In situ* and bedding corrected distribution of the susceptibility axes. B: Bedding plane. b) Anisotropy degree (P) vs. average susceptibility (Km). c) Anisotropy degree (P) vs. shape parameter (T). d) Foliation vs. lineation, Flinn's diagram (Jelinek, 1981).

calculated from the bedding corrected VGP is SR: 8.6°N 355.3°E $A_{95}=10.1°$ K = 26.78 N = 9 (Fig. 9). This paleomagnetic pole passes at least 3 of the reliability criteria of Van der Voo (1990): i) the age of the unit is well known; ii) the specimens were submitted to detailed demagnetizations and iii) the paleomagnetic pole does not coincide with others of younger age.

4.3. Baritú Formation

The initial susceptibility is between 5.8 and 7.5×10^{-5} (SI) and the NRM intensities between 1.596 and 2.284 mA/m. Specimens were not saturated up to 2000 mT during the acquisition of the IRM, typical of hematite (Fig. 4c). In the back field curves 2 phases with different coercitivities can be identified (Fig. 4c). Demagnetization curves show unblocking temperatures close to 600 °C (Ti?-hematite) and 680 °C (hematite) (Fig. 10). In 3 specimens a low-temperature component (A) was isolated. A high-temperature component (B) was obtained in most samples. No tilt or fold test was applied since all samples were collected from the same succession with identical bedding attitude. Component B shows a good directional consistency and a mean was obtained from the *in situ* direction, which does not coincide with any expected post-Devonian South American direction. A mean VGP was calculated from the bedding corrected specimen remanence direction PoC: 65.9°S 306.6°E $A_{95}=6.8°$ K = 66.45 n(specimens) = 8 (Table 5 and Fig. 6c). This paleomagnetic pole position is consistent with that recently obtained from the Devonian Achala granitoid in central Argentina (Geuna et al., 2008) (Fig. 7).

5. Interpretation of the Early Paleozoic paleomagnetic data from NW Argentina

5.1. Previous interpretations in view of the new data

Spagnuolo et al. (2008) published the first paleomagnetic pole for the Campanario Formation. The result came from a single locality at Matancillas and showed a large clockwise rotation respect to different

Table 4
Average magnetic direction of Santa Rosita Formation. St: Strike. (*) Bedding corrected data. K and α_{95}: statistical parameters of Fisher (1953). Lat: latitude; (−): south latitude. Long: longitude.

Sample	D (°)	I (°)	MAD/ α_{95}	Bedding		D (°) (*)	I (°) (*)	VGP *in situ*		VGP (*)	
				St (°)	Dip (°)			Lat	Long	Lat	Long
IRU 23 (n = 5)	116.9	37.7	15.2	234	45	64.3	68.8	−31.9	13.6	−3.5	328.7
IRU 24 (n = 4)	111.5	31.4	24.5	234	45	71.1	61.6	−25.9	16.6	−2.5	339.1
CAS 01 (n = 9)	83.4	3.3	2.1	204	55	65.3	47.5	5.4	20.8	8.5	348.6
SA 04 (n = 4)	80.6	12.0	3.9	226	29	71.6	26.9	6.2	15.7	10.6	4.3
SA 05 (n = 3)	80.5	21.0	4.5	226	29	66.6	34.8	4.3	11.2	12.4	357.6
SA 06 (n = 3)	66.5	7.3	8.5	226	29	60.6	16.3	19.9	11.7	22.9	4.3
SA 07 (n = 5)	79.7	14.5	2.3	226	29	69.4	28.7	6.4	14.1	12.0	2.4
SA 08 (n = 2)	79.7	8.0	12.6	226	29	72.6	22.9	7.8	17.2	10.8	6.9
SA 02 (n = 4)	82.6	19.0	35.5	232	17	76.2	26.9	17.4	3.1	4.3	6.0
Mean	Dec = 85.6° Inc = 17.6° α_{95} = 12.1° K = 18.98 R = 8.58 N = 9										
	Dec* = 68.9° Inc* = 37.0° α_{95}* = 12.0° K* = 19.34 R* = 19.34										
Mean VGP's*: Lat: 8.6°N Long: 355.3°E A_{95} = 10.1° K = 26.78											

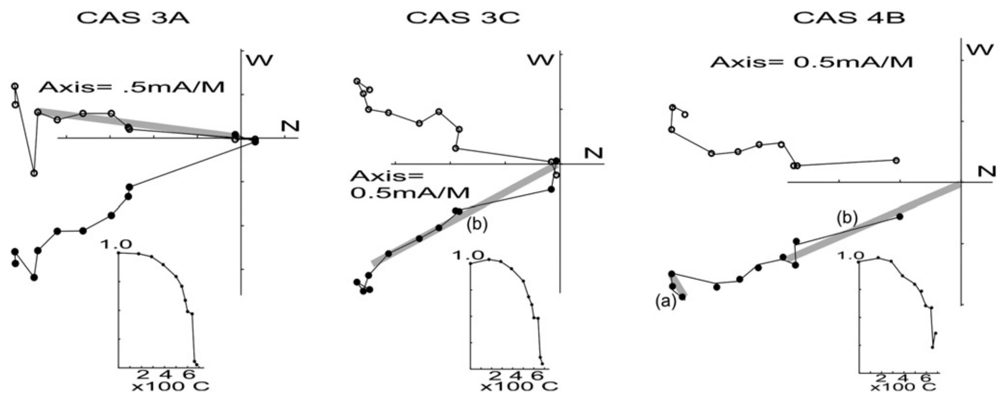

Fig. 10. Representative demagnetization behavior of analyzed specimens (geographic coordinates) of the Baritú Formation. In the vector diagram, closed (open) symbols represent projections on the horizontal (vertical) plane.

coeval reference poles for Gondwana (Grunow and Encarnación, 2000; Meert et al., 2001; McElhinny et al., 2003; Fig. 7) that was interpreted as an Andean tectonic rotation associated to the Bolivian Orocline (Spagnuolo et al., 2005) along an E–W transfer zones on the Andean margin (Spagnuolo et al., 2008). This interpretation was the most conservative giving the lack of further paleomagnetic data from other units in the same locality and the same unit in other localities.

Our new results from the Campanario Formation provide data from a locality situated over 35 km to the west from the first one and yielded almost identical results. The new pole can be calculated with more than twice the number of original specimens. Therefore our result provides significant confidence to consider the data representative of the Campanario Formation in a large area.

With this new result the three explanations previously suggested (see the introduction) are still valid, but some seem more likely than before. A further constraint is now provided by the paleomagnetic pole from the Santa Rosita Formation. It must be taken into consideration that one of the sampling localities of the Santa Rosita Formation corresponds to Matancillas, at the exact location where the first study of the Campanario Formation (Spagnuolo et al., 2008) was carried out. The paleomagnetic pole of the Ordovician unit shows a very reduced rotation value. This is in part due to the reference Gondwana pole which moves eastward from 495 to 475 Ma (see Fig. 7), but the Campanario and the Santa Rosita poles are significantly different allowing to infer that a common age of magnetization for both is unlikely. Moreover, no reversals have been found in the latter, consistent with an Early Ordovician age, while some reversals, consistent with a Late Cambrian magnetization age (Pavlov and Gallet, 1998) have been recorded in the Campanario Formation at both localities. Despite possible inclination error in some samples of the Santa Rosita Formation, declination values from all localities are very consistent and suggest that no relative rotations have occurred between these localities since remanence was acquired. The preliminary mean geomagnetic pole from the Baritú Formation does not show any significant rotation either.

The model of a large Andean rotation that affected the sampling area at Matancillas to explain the anomalous position of the original pole for the Campanario Formation (Spagnuolo et al., 2008) may still hold but has been severely weakened by the new paleomagnetic data. In the first place, Andean rotations well over 30° are rare along the Bolivian Orocline (Somoza et al., 1996; Beck, 1998; Randall, 1998, Fig. 11a), particularly so far inboard from the continental margin. The new data indicate that localities situated at around 35 km would have undergone identical rotations due to the Andean Orogeny. More difficult to explain is the fact that the Early Ordovician units show a rotation significantly smaller. Preliminary data from Devonian rocks (Baritú Formation) also show lack of significant rotations. Thus, unless we consider the paleomagnetic data from the Santa Rosita Formation unreliable (due to lack of a definite field test), it looks unlikely that the Late Cambrian pole could be significantly different than the Early Ordovician one. Therefore, if the anomalous pole position of the Campanario Formation is to be explained by a tectonic rotation, most of it must have occurred before deposition of the Santa Rosita Formation and cannot be attributed to the Andean Orogeny.

Table 5
Magnetic components of Baritú Formation. (*) Bedding corrected data. K and α_{95}: statistical parameters of Fisher (1953). Lat: latitude; (−): south latitude. Long: longitude. (A)/(B): component of low/high temperature.

Sample	Specimen	D (°)	I (°)	MAD/α_{95} (°)	Bedding		D (°) (*)	I (°) (*)	VGP	
					Strike (°)	Dip (°)			Lat	Long
CAS 3	3 B-b (b)	155.4	−12.2	5.8	232	78	171.3	62.4	−68.6	312.3
	3 B-b (a)	12.8	−7.2	4.4	232	78	51.4	−39.7		
	3 A (b)	151.9	−6.6	4.7	232	78	170.4	69.0	−60.1	306.7
	3 C (b)	152.5	−16.3	7.7	232	78	162.4	59.9	−67.3	331.2
	3 D (b)	152.6	−11.5	5.6	232	78	166.5	64.3	−64.9	317.3
Mean CAS3 (B)	153.1	−11.7	4.8	K = 361.65	n = 4	167.4	63.9	−65.5	316.2	
CAS 4	4 D (b)	155.9	−21.1	9.4	232	78	164.5	54.2	−72.4	341.6
	4 A (b)	157.9	−6.5	5.4	232	78	183.3	65.7	−65.4	289.6
	4 A (a)	63.5	−16.0	9.8	232	78	70.2	7.5		
	4 B (b)	157.9	−6.1	6.6	232	78	184.0	66.0	−65.0	288.6
	4 C (a)	77.6	−12.5	12.9	232	78	70.8	21.6		
	4 C (b)	154.3	0.4	7.0	232	78	189.3	73.2	−54.0	286.7
Mean CAS4 (B)	156.5	−8.3	10.5	K = 77.01	n = 4	178.0	65.1	−65.6	296.7	
Specimens mean	Dec = 154.8° Inc = − 10.0° α_{95} = 4.9° K = 129.52 R = 7.95 n = 8									
	Dec* = 172.6° Inc* = 64.6° α_{95}* = 4.9° K* = 129.52 R* = 7.95									
Mean VGP's (specimens): Lat: 65.9°S Long: 306.6°E A_{95} = 6.8° K = 66.45 n = 8										

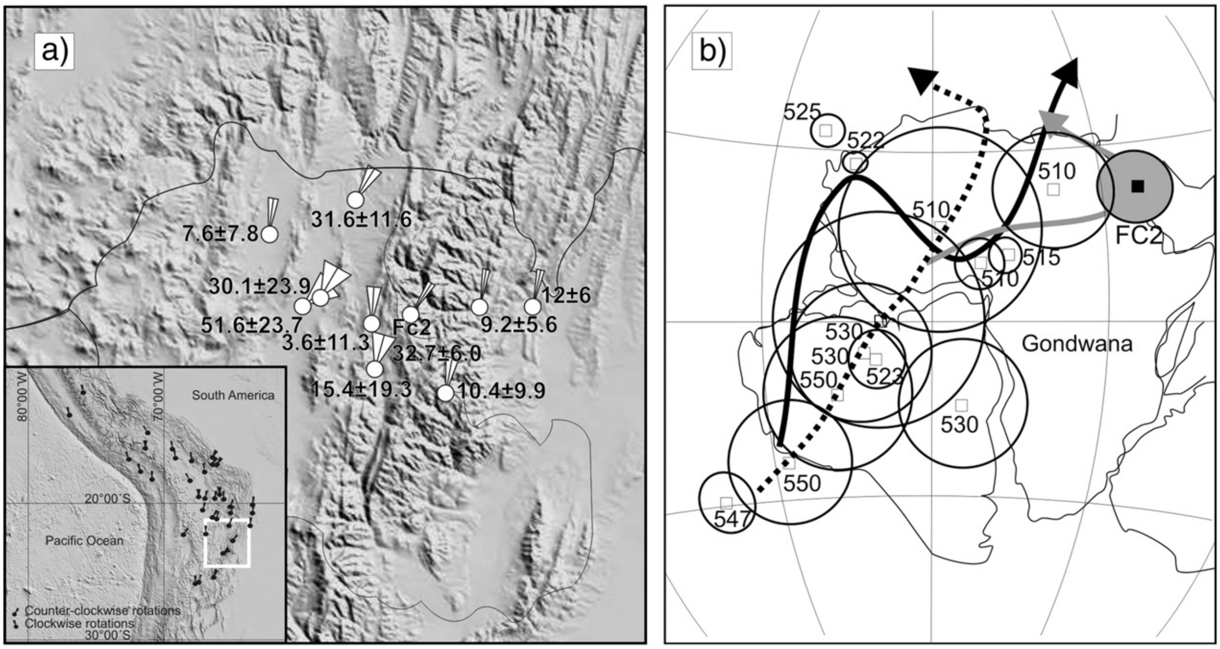

Fig. 11. Previous models explaining the rotations found in the Campanario Formation. See the text for a more complete explanation. a) Central Andean Rotational Pattern (Coutand et al. 1999; Reynolds et al., 2001; Prezzi et al., 2004; Maffione et al., 2009; Hernández et al., 1996; Spagnuolo et al., 2008). b) A more complex APWP. Gray (Spagnuolo et al., 2008), black (Trindade et al., 2004), dotted (Meert and Van der Voo, 1996).

The arguments presented above suggest that with the present database the hypothesis that holds better is that the Campanario and the Santa Rosita poles are representative of the Pampia terrane. In most tectonic models (e.g. Ramos et al., 2010 and references therein) by the Late Cambrian the Pampia terrane was already an integral part of Gondwana. In such case, the paleomagnetic poles of the Campanario and Santa Rosita Formations should be representative of Gondwana. However, the anomalous position of the Campanario pole would imply that the APWP of this supercontinent should be longer and more complex than proposed in the last two decades (see Meert, 2003 and references therein). This has already been discussed by Spagnuolo et al. (2008) who argued that modifying the Cambrian APWP for Gondwana (Meert and Van der Voo, 1996; Grunow, 1999; Meert et al., 2001; Trindade et al., 2006; Fig. 11b) to allow for the Campanario pole (look that the Santa Rosita pole would fit relatively well the already accepted path) would imply an extremely fast track from northern Africa at 510 Ma to the Red Sea in 500 Ma, coming back to the north of Africa at ca. 490 Ma. This kind of displacement implies very high speeds of the order of at least 30 cm/year (Fig. 11b), close to the fastest continental drift ever proposed (Gordon, 1991; Gurnis and Torsvik, 1994; Evans, 1998; Sánchez Bettucci and Rapalini, 2002; Trindade et al., 2004, 2006). According to these authors maximum speed of continental plates has been suggested from 11 up to 38 cm/year. Only with new coeval and consistent paleomagnetic data from other regions in South America or other continents this hypothesis can be validated.

5.2. Pampia: a displaced terrane from Kalahari?

Most evidence suggests that the paleopole of the Campanario Formation (FC2) is representative of the Pampia terrane (Ramos, 1988; Rapela et al., 1998a, b). As exposed above, the rotation found in the Late Cambrian sediments may have occurred near the Cambrian–Ordovician boundary.

The third alter006Eative, already discussed by Spagnuolo et al. (2008), is that the paleomagnetic data obtained so far indicates a relative displacement between Pampia and the Rio de la Plata craton, already part of Gondwana, during the latest Cambrian. Taking into consideration different average poles of Gondwana of 500–485 Ma and the paleopole of Pampia (in African coordinates according to the reconstruction of Reeves et al., 2004), a clockwise rotation of 46° around an Euler pole at 10.1°S 19.5°E would match both paleomagnetic poles (Fig. 12a). When applied to the continents, this rotation places Pampia near the southern border of Kalahari (Fig. 12a).

Whitmeyer and Simpson (2003), Schwartz and Gromet (2004), Rapela et al. (2007) and Drobe et al. (2009) suggested movements to the north (present coordinates) over a transform margin located between Pampia plus other small blocks and the rest of Gondwana, until Early Ordovician times. The formation of the Mozambique belt and the Ross–Delamerian Orogen due to the collision and final assembly of Antarctica, Kalahari and other blocks in southern Gondwana, may have generated the displacement of small fragments by escape tectonic along the southwestern Gondwana margin until the Ordovician, in a similar deformational style to the formation of the Himalayas by the India–Asia collision (Porada and Berhorst, 2000; Ring et al., 2002; Jacobs and Thomas, 2004; Vaughan and Pankhurst, 2008).

Recently, Rapela et al. (2007) published a geotectonic model in which Pampia, considered here as the basement upon which the Puncoviscana sedimentary succession was deposited, underwent a major displacement from southern Kalahari along the western border of the Rio de la Plata craton in Cambrian times. These sediments, that formed the Puncoviscana basin were, according to this model, the product of denudation of the orogens generated by the collision of Kalahari with the Rio de la Plata and Antarctica since ~550 Ma. In that moment, the approach and subsequent collision of an allochthonous block composed by the Western Pampean Ranges, Amazonia and Arequipa–Antofalla generated the magmatic arc along the Pampean Orogen (540–520 Ma) followed by major dextral strike-slip movements.

A major change in the crustal electrical resistivity character has been found between Pampia and the Rio de la Plata craton from magnetotelluric studies by Favetto et al. (2008). This geophysical evidence has confirmed the different origin of both crustal blocks. These authors have placed the “suture” between them very close to the foothills of the Sierras de Córdoba (Eastern Pampean Ranges). A recent gravimetric transect by Ramé and Miró (2010) has also found evidence of a major crustal discontinuity at approximately the same

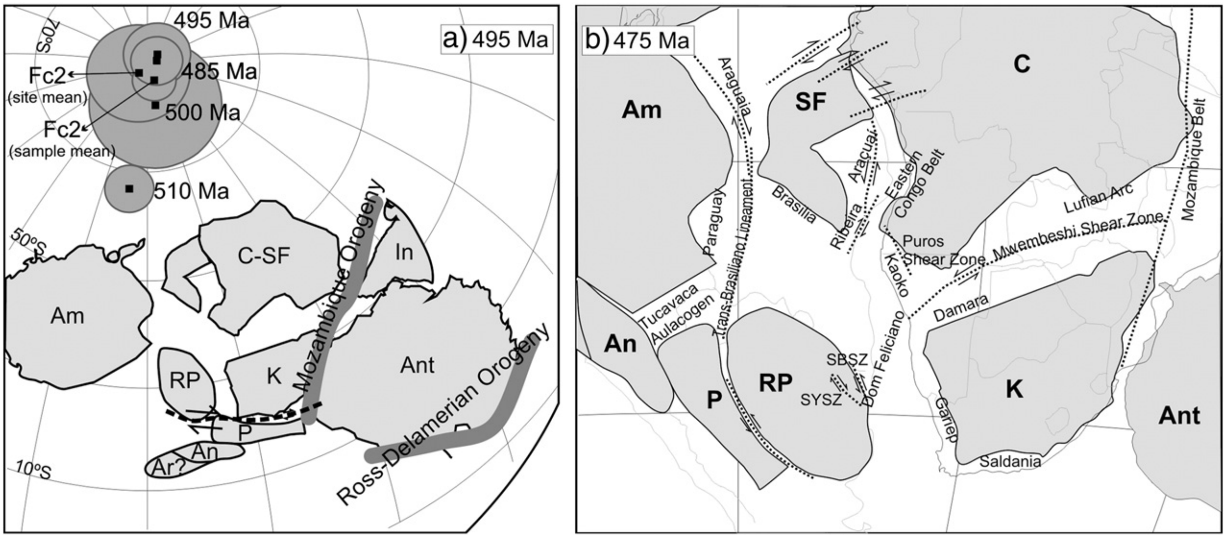

Fig. 12. Paleogeographic evolution of the SW Gondwana between Lower Cambrian and Middle Ordovician and the paleomagnetic poles that were used: Campanario Formation (Fc2, this work), 485 (McElhinny et al., 2003), 495 (Grunow and Encarnación, 2000), 500 (Meert et al., 2001) and 510 Ma (McElhinny et al., 2003). a) 495 Ma. P: Pampia, Ar: Arequipa, An: Antofalla, Am: Amazonia, C–SF: Congo–San Francisco, In: India, Ant: Antarctica, K: Kalahari, RP: Rio de la Plata. b) 475 Ma. SYSZ: Sarandí Yi Shear Zone; SBSZ: Sierra Ballena Shear Zone.

location. However, their model cannot account for any obducted oceanic crust and the authors have proposed the presence of a high-angle shear zone instead. These recent geophysical findings strongly suggest that the major boundary zone between the Rio de la Plata and Pampia blocks lies below the Cenozoic cover of the Chaco-Pampean plains and that the transpressive shear zones well exposed along the Pampean Ranges in Córdoba (Martino, 2003; Simpson et al., 2003) are probably subsidiary fault zones to the major shear one that marks the boundary between both terranes.

According to the detrital zircon ages found in the protoliths of metasediments of the Pampean Belt (main peaks at ~600 Ma and ~1100 Ma and a small fraction of ~1900 Ma) and the Puncoviscana Formation (1700 Ma, 1150–850 Ma and 650–520 Ma) a conspicuous lack of zircons with the diagnostic age of the Rio de la Plata basement (2100–2300 Ma) is characteristic of Pampia (Rapela et al., 1998b; Schwartz and Gromet, 2004; Rapela et al., 2007; Adams et al., 2008a; Hauser et al., 2011). This suggests that a direct collision between Pampia and the western margin of the Rio de la Plata craton is not likely before the Late Cambrian (Rapela et al., 1998b; Schwartz and Gromet, 2004; Rapela et al., 2007; Adams et al., 2008a; Collo et al., 2009). Collo et al. (2009) proposed an evolution of the Pampean Ranges during the Late Proterozoic Brasiliano Cycle, in which an oceanic plate subducted under a Mesoproterozoic terrane (named as Córdoba Terrane) generating the Brasiliano magmatism of the Eastern Pampean Ranges, with the collision of an unidentified Paleoprotezoic craton occurring ca. 640–600 Ma. This interpretation is compatible with the model proposed here if the Paleoproterozoic craton is considered to be Kalahari. In this model, the Puncoviscana basin opened after this tectonic event accumulating thousands of meters of clastic sediments plus minor extensional magmatism. Between ~550 and 530 Ma the Puncoviscana basin was closed and inverted with the subduction of oceanic crust and the generation of the Pampean Magmatic Arc characterized by metaluminous calc-alkaline granitoids of ~535 Ma and rhyolites–dacites along the Eastern Pampean Ranges at around 530 Ma (Rapela et al., 1998a,b). The age of the Pampean Orogen has been dated at 515–520 Ma (U–Pb in monazite, Gromet and Simpson, 1999), 490 $\pm$ 2 Ma (cooling ages; Fantini et al., 1998) and 502 $\pm$ 5 Ma (Ar–Ar; Krol and Simpson, 1999). All these ages indicate that the Pampean Orogen was active until the Late Cambrian (Simpson et al., 2003; Mulcahy et al., 2007). U–Pb geochronological studies in the Sierra Norte of Córdoba indicate that calcalkaline magmatism occurred between 550 and 525 Ma while the peraluminous magmatism took place between 525 and 515 Ma (Miró et al., 2005). Closure of the Puncoviscana basin was associated with obduction of ophiolite, generation of granulite and migmatite, crustal thickening, peraluminous magmatism (Rapela et al., 1998a, b) and development of major dextral shear zones and regional foliations of Late Cambrian–Early Ordovician ages (Rapela et al., 1998b; Martino, 2003; Miró et al., 2005; Schwartz et al., 2008).

Because the Pampean belt is characterized by low-P–high-T anatectic rocks until 509 Ma (Rapela et al., 1998a,b; Simpson et al., 2003), some authors have proposed that this orogen was not a collisional one but the result of the subduction of an oceanic ridge (Simpson et al., 2003; Miró et al., 2005; Piñán Llamas and Simpson, 2006; Schwartz et al., 2008). However, those characteristics may also be applied to transpressive orogens (Konopásek et al., 2005).

Hongn and Mon (1999) and Hongn et al. (2010) suggested a metamorphic episode of high-T and low-P at around 500 Ma affecting NW Argentina and N Chile (Lucassen et al., 1996; Becchio et al., 1997). This episode has been interpreted either as a rift associated to thermal anomalies related to an extensional regime ("the collapse of the Tilcaric Orogeny", Omarini and Sureda, 1994) or a compressional event (Hongn and Mon, 1999) indicating the last phases of the tangential accommodation of Pampia and the Rio de la Plata craton and the backward jump of the trench and initiation of a new subduction process.

According to Piñán Llamas and Simpson (2006) and Schwartz et al. (2008) the subduction of a mid-ocean ridge under the Río de la Plata craton generated a relative change in the motion of the plates that moved from orthogonal or oblique to parallel. The model proposed here is compatible with such change. In the Guamanes zone (Sierras de Córdoba) it can be seen a re-orientation of the fabric at 515 Ma, suggesting a change in the compressional regime from orthogonal to the margin to a largely dextral strike slip displacement (Simpson et al., 2003). This transpressive regime was mainly accommodated as transcurrent movements along shear zones located in the boundary between the Paleoproterozoic (Kalahari–Rio de la Plata) and the Mesoproterozoic (Pampia) crusts (Martino, 2003; Vaughan and Pankhurst, 2008) during Cambrian times.

Detrital zircons from the Middle to Late Cambrian Mesón Group (Adams et al., 2008b) show major peaks at 530–519 Ma, 700–560 Ma and 1000–900 Ma (similar to the detrital zircon ages of the

Puncoviscana Formation), plus a pick of 502 Ma interpreted as associated with the beginning of the Famatinian magmatism and likely indicating the sedimentation age. A small (11%) but significant new group of 2200–1980 Ma, may indicate a provenance from the Rio de la Plata craton. The presence of this Paleoproterozoic group marks the main difference between the source areas of the Puncoviscana Formation and the Mesón Group, suggesting a closer position of Pampia to Río de la Plata, Amazonia or Arequipa blocks (e.g. Loewy et al., 2003; Schwartz and Gromet, 2004). A provenance study in the basement of the Famatina Ranges (Collo et al., 2009) indicates detrital zircon ages for the Cambrian Negro Peinado Formation of 515–530 Ma, 1030–960 Ma and 1180–1245 Ma with no Paleoproterozoic contribution, while the Early Ordovician Achavil Formation shows Neoproterozoic peaks and a subordinated contribution of Paleoproterozoic grains (1908–2097 Ma), very similar to the pattern found in the Mesón Group in the northern areas of Pampia. These findings of Paleoproterozoic ages were interpreted as the proximity of the Río de la Plata craton as a source area (Rapela et al., 2007; Collo et al., 2009). It is interesting that the older "Rio de la Plata" signature appears for the first time in younger rocks as we move south along Pampia, consistent with a progressive displacement of Pampia towards the north (present day coordinates) along the border with the Rio de la Plata craton.

In the southern margin of Antarctica, the Ross–Delamerian orogeny developed between 515 and 490 Ma (Boger and Miller, 2004; Cawood and Buchan, 2007; Vaughan and Pankhurst, 2008). This new convergent margin was emplaced all around the southern margin of Gondwana and was defined by Cawood (2005) as Terra Australis. This orogeny generated the youngest collisional events of Gondwana assembly and produced a major reorganization in the plate movements (Boger and Miller, 2004; Jacobs et al., 2006; Boger, 2011). Fig. 5 of Boger and Miller (2004) shows that the collision of India–Antarctica against Kalahari could have triggered tectonic escape of Pampia towards the northwest (present-day coordinates), moving from a position close to southern Kalahari into its final location next to the Río de la Plata. This movement must have taken place along a major or several transcurrent (or transform) faults (Fig. 12). The Saldania Orogeny took place in Kalahari between 550 and 500 Ma (Germs, 1995; Rozendaal et al., 1999) and was correlated with the Pampean Orogeny (Cawood and Buchan, 2007: Rapela et al., 2007) or the Ross–Delamerian Orogeny (Rozendaal et al., 1999; Da Silva et al., 2000). The absence of collisional characteristics suggests that it developed in a strike-slip regime with large shear zones which displayed episodes of successive sinistral and dextral movements (Rozendaal et al., 1999). Even more, Rozendaal et al. (1999) suggested the presence of different allochthonous terranes in South Africa emplaced by sinistral transpression of the Ross–Delamerian Orogeny (Da Silva et al., 2000).

Boger and Miller (2004) proposed that collision between India–Antarctica and Eastern Gondwana occurred between 530 and 510 Ma with the last phases of deformation and magmatism occurring at 500–490 Ma. These authors suggested that the decreasing speed between these two continental masses generated changes in the magnitude and directions of the plate movements at a global scale. This picture is basically compatible with our interpretation that the paleomagnetic poles form the Campanario and Santa Rosita formations reflect the movement of Pampia relative to the Rio de la Plata craton and other Gondwana blocks. The consistent pole of the Santa Rosita Formation suggests that by ~485 Ma most of this displacement due to tectonic escape of Pampia had ended.

Strike-slip displacement of Pampia occurred until final docking against Amazonia, in the north (present-day coordinates). Boundary between these two crustal blocks probably lies within the Chiquitos–Tucavaca orogen. A thick sedimentary pile was deformed here between the Early Cambrian (Ramos, 2008) and the latest Cambrian–Early Ordovician (500–480 Ma; Trompette et al., 1998; Tohver et al., 2006). Because geometry of the northern boundary of Pampia is not well established due to the thick Cenozoic sedimentary cover, the precise kinematics of docking remains unknown. More to the northeast, in the Ediacaran Itapucumí Group (W Río Apa craton), Campanha et al. (2010) described a mobile belt associated to a Late Brasilian–Panafrican deformation during the Late Cambrian. These authors interpreted it as related to the last collisional events of Amazonia against Gondwana along the Pampean Belt. This could well be related to the final docking processes of Pampia. Moreover, in the Paraguay belt there is Cambrian deformation and remagnetization that was followed by large rotations about vertical axes and regional metamorphism at about 495 Ma (Tohver et al., 2010).

Pampia has been correlated by some authors with the Arequipa–Antofalla block (Sims et al., 1998; Lucassen et al., 2000; Rapela, 2000; Bahlburg et al., 2000; Kleine et al., 2004; Steenken et al., 2004; Casquet et al., 2006; Collo et al., 2009). Very similar isotopic compositions of their basements and detrital zircon ages plus the absence of a major suture between them are important arguments in favor of this idea. Forsythe et al. (1993) obtained a paleomagnetic pole in the Choschas Granite (502 ± 10 Ma) in the Almeida Ranges (N Chile), which corresponds to the Antofalla block. When this pole is compared with the coeval average pole of Gondwana major declination and inclination anomalies are observed (Rapalini et al., 1999). Since the rotation observed is counterclockwise, it cannot be directly assigned to the Central Andean rotation pattern (CARP, Somoza et al., 1996). Furthermore, Late Ordovician to Silurian paleomagnetic results from the same region do not reproduce the inclination and declination anomalies, while the Early Ordovician results (Forsythe et al., 1993; Rapalini et al., 2002) only show an anomaly in declination.

If the Arequipa–Antofalla block is placed attached to Pampia according to the Late Cambrian paleomagnetic pole for the latter the colatitude band associated to the Choschas pole coincides with the coeval average poles of Gondwana eliminating the inclination anomaly already mentioned (Fig. 13). This result suggests that Pampia and Arequipa–Antofalla moved together from a position at the southern margin of Kalahari (present coordinates) in the Middle–Late Cambrian to its present position respect to the Rio de la Plata craton in Early Ordovician times. The movement was the product of the tectonic escape of fragments of the Kalahari craton due to the

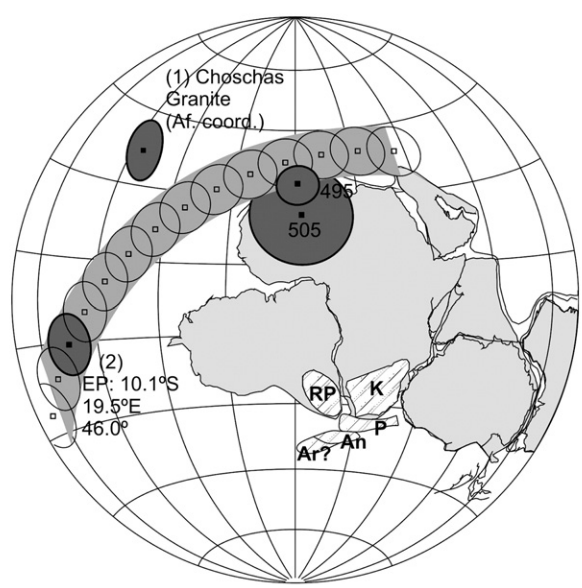

Fig. 13. Average paleomagnetic poles of Gondwana of 495 (Grunow and Encarnación 2000) and 505 (Meert et al., 2001) Ma. Paleomagnetic pole of Choschas Granite in African coordinates (1) and after rotation around the 10.1° 19.5° 46.0° Euler Pole (2). In light gray it is shown the colatitude band associated to the Choschas pole. The position of the Pampia and Antofalla (−Arequipa?) terranes are according to the same Euler pole. RP: Río de la Plata. K: Kalahari. P: Pampia. An: Antofalla. Ar: Arequipa.

major collision with Antarctica in Cambrian times. It is interesting to note that other, minor blocks were also displaced along major strike slip zones between the Kalahari and Rio de la Plata craton. The Punta del Este terrane (Preciozzi et al., 1999; Basei et al., 2000), interpreted as a fragment of the Kalahari craton, underwent a major sinistral displacement relative to the Rio de la Plata craton along the Sierra Ballena and possibly the Alferez Cordillera shear zones (Uruguay) during Cambrian to Early Ordovician (?) times. Therefore, final amalgamation of Kalahari and Antarctica to Gondwana produced major displacements of peripheral tectonic blocks during last stages of Gondwana assembly in Cambrian and Early Ordovician times.

Whether the Arequipa–Antofalla is a single or composite block (Bahlburg and Hervé, 1997; Loewy et al., 2003; Rapalini, 2005; Ramos, 2008), is still a matter of debate and exceeds the scope of this paper. The paleomagnetic constraints for Arequipa–Antofalla strictly apply to the southern Antofalla block, so that whether the whole block, as depicted in Fig. 13, or a more reduced one traveled from southern Kalahari attached to Pampia is not constrained by our model.

6. Conclusions

A paleomagnetic study was carried out in a new locality for the Late Cambrian Campanario Formation, previously studied by Spagnuolo et al. (2008). This was complemented with the paleomagnetic study of the Early Ordovician Santa Rosita Formation at four localities, while preliminary data was obtained for the overlying Devonian Baritú Formation. All these units are exposed in NW Argentina. A pre-tectonic high temperature magnetic component carried by hematite, that passes a reversal test, was isolated in the Campanario Formation. Merging the new results with those from the previous study a new paleomagnetic pole was calculated for this units (FC2) at 1.5°N 1.9°E ($A_{95}=9.2°$ $K=37.46$ $N=8$ sites), which is basically identical to the previous one and it is anomalous respect to the Late Cambrian reference pole of Gondwana. The paleopole obtained in the Santa Rosita Formation (8.6°N 355.6°E $A_{95}=10.1°$ $K=26.78$ $N=9$ samples) in three localities is consistent with the coeval reference pole for Gondwana and constrain the rotation to the Late Cambrian–Early Ordovician. Rotated paleomagnetic positions obtained from two well separated localities and the age constraints suggest that a local tectonic rotation is unlikely and that the poles are representative of the whole of Pampia. We suggest that a significant displacement of Pampia with respect to other adjacent Gondwana blocks and cratons may explain the paleomagnetic results simpler than a large change in the APWP of Gondwana, which would need very high absolute drifting speeds.

We propose a simple kinematic model in which the Pampia and Antofalla (−Arequipa?) blocks moved in Cambrian times from a position at the present southern border of the Kalahari craton, along a major or several transcurrent faults into its final positions next to the Rio de la Plata craton by the Early Ordovician. The cause of such displacement is related to the Mozambique and the Ross–Delamerian Orogenies, associated to the final assembly of Kalahari and Antarctica into Gondwana. This would have generated a global reorganization of tectonic plates and tectonic escape of blocks like Pampia along the free continental margins. This model can better explain several geochronologic and paleomagnetic data as well as other existing geological features.

Acknowledgements

SuperIapd 2000 (Torsvik et al., 2000), GMAP (Torsvik et al., 2000), Paleomagnetism Data Analysis v.4.2 (Enkin, 1994) and Anisoft 4.2 (Chadima and Jelinek, 2008) software packages were used to analyze data. This study was supported through grants by Universidad de Buenos Aires UBACyT X2183 and ANPCyT PICT-1074 to A.E. Rapalini and it is part of the PhD thesis of C.M. Spagnuolo (University of Buenos Aires). CONICET (Argentine Research Council) is acknowledged for doctoral and post-doctoral fellowships to C.M. Spagnuolo. Comments by reviewers S. Pisarevsky and an anonymous one and guest editor R. Trindade highly improved the final version.

References

Aceñolaza, G., Aceñolaza, F.G., 2002. Ordovician trace fossils of Argentina. In: Aceñolaza, F.G. (Ed.), Aspects of the Ordovician System in Argentina. INSUGEO: Correlación Geológica, 16, pp. 177–194.

Aceñolaza, F.G., Toselli, A.J., 1981. Geología del Noroeste Argentino. Facultad de Ciencias Naturales e Instituto Miguel Lillo, Universidad Nacional de Tucumán, Publicación Especial 1287, 1–212.

Adams, C.J., Miller, H., Toselli, A.J., Griffin, W.L., 2008a. The Puncoviscana Formation of Northwest Argentina: U–Pb geochronology of detrital circons and Rb–Sr metamorphic ages and their bearing on its stratigraphic age, sediment provenance and tectonic setting. Neues Jahrbuch fur Geologie und Palaontologie 247 (3), 341–352.

Adams, C.J., Miller, H., Aceñolaza, G.F., Toselli, A.J., 2008b. Cambrian paleogeography at the western Gondwana margin: U–Pb ages and provenance areas of detrital zircons of the Mesón Group (Upper Cambrian), Northwest Argentina. 7° International Symposium on Andean Geodynamics (ISAG, Nice). Resúmenes extendidos, pp. 17–20.

Astini, R.A., 2003. The Ordovician Proto-Andean Basins. In: Benedetto, J.L. (Ed.), Ordovician Fossils of Argentina. : Secretaría de Ciencia y Tecnología. Universidad Nacional de Córdoba, Argentina, pp. 1–74.

Astini, R.A., 2008. Sedimentación, facies, discordancias y evolución paleoambiental durante el cambro-ordovícico. Relatorio de la geología y recursos Naturales de la Provincia de Jujuy. Asociación Geológica Argentina, Buenos Aires. 50–73.

Augustsson, C., Rusing, T., Adams, C.J., Chmiel, H., Kocabayoglu, M., Buld, M., Zimmermann, U., Berndt, J., Kooijman, E. Detrital quartz and zircon combined: the production of mature sand with short transportation paths along the Cambrian west Gondwana margin, NW Argentina. Journal Sedimentological Research, submitted for publication

Bahlburg, H., Hervé, F., 1997. Geodynamic evolution and tectonostratigraphic terranes of northwestern Argentina and northern Chile. Geological Society of America Bulletin 109, 869–884.

Bahlburg, H., Moya, M.C., Zimmermann, U., Bock, B., Hervé, A.F., 2000. Paleozoic plate tectonic evolution of the Western Gondwana margin in northern Chile and Northwestern Argentina. International Geological Congress, pp. 345–353.

Baldis, B.A.J., Gorroño, A., Ploszkiewicz, J.V., Sarudiansky, R.M., 1976. Geotectónica de la Cordillera Oriental, Sierras Subandinas y comarcas adyacentes. Actas 6° Congreso Geológico Argentino, 1, pp. 3–22.

Basei, M.A.S., Siga Jr., O., Masquelin, H., Harara, O.M., Reis Neto, J.M., Preciozzi, F., 2000. The Dom Feliciano Belt of Brazil and Uruquay and its foreland domain, the Rio de la Plata Craton. In: Cordani, U.G., Milani, E.J., Thomaz Filho, A., Campos, D.A. (Eds.), Tectonic Evolution of South America, pp. 311–334.

Becchio, R., Lucassen, F., Franz, G., Viramonte, J., 1997. Condiciones de P–T del basamento metamórfico de alto grado. Borde oriental de la Puna Austral Argentina: Actas 8° Congreso Geológico Chileno, 2, pp. 1220–1224. Antofagasta.

Beck, M.E., 1998. On the mechanism of crustal block rotations in the central Andes. Tectonophysics 299, 75–92.

Boger, S.D., 2011. Antarctica — before and after Gondwana. Gondwana Research 19, 335–371.

Boger, S.D., Miller, J. McL, 2004. Terminal suturing of Gondwana and the onset of the Ross–Delamerian Orogeny: the cause and efect of an Early Cambrian reconfiguration of plate motions. Earth and Planetary Science Letters 219, 35–48.

Buatois, L.A., Mángano, M.G., 2003. Sedimentary facies, depositional evolution of the Upper Cambrian–Lower Ordovician Santa Rosita formation in northwest Argentina. Journal of South American Earth Sciences 16, 343–363.

Campanha, G.A.da C., Warren, L., Boggiani, P.C., Grohmann, C.H., Cáceres, A.A., 2010. Structural analysis of the Itapucumí Group in the Vallemí region, northern Paraguay: evidence of a new Brasiliano/Pan-African mobile belt. Journal of South American Earth Sciences 30 (1), 1–11.

Casquet, C., Pankhurst, R.J., Fanning, C.M., Baldo, E., Galindo, C., Rapela, C.W., González-Casado, J.M., Dahlquist, J.A., 2006. U–Pb SHRIMP zircon dating of Grenvillian metamorphism in Western Sierras Pampeanas (Argentina): correlation with the Arequipa–Antofalla craton and constraints on the extent of the Precordillera Terrane. Gondwana Research 9 (4), 524–529.

Cawood, P.A., 2005. Terra Australis Orogen: Rodinia breakup and development of the Pacific and Iapetus margins of Gondwana during the Neoproterozoic and Paleozoic. Earth Science Reviews 69, 249–279.

Cawood, P.A., Buchan, C., 2007. Linking accretionary orogenesis with supercontinent assembly. Earth Science Review 82, 217–256.

Chadima, M., Jelinek, V., 2008. Anisoft 4.2. Beta-version.

Chernicoff, C.J., Zappettini, E.O., 2003. Delimitación de los terrenos tectonoestratigráficos de la región centro-austral Argentina: evidencias aeromagnéticas. Revista Geologica de Chile 30 (2), 299–316.

Collo, G., Astini, R.A., Cawood, P.A., Buchan, C., Pimentel, M., 2009. U–Pb detrital zircon ages and Sm–Nd isotopic features in low-grade metasedimentary rocks of the Famatina belt: implications for late Neoproterozoic–early Palaeozoic evolution of the proto-Andean margin of Gondwana. Journal of the Geological Society 166 (2), 301–318.

Cordani, U., Sato, K., Teixeira, W., Tassinari, C.C.G., Basei, M.A.S., 2000. Tectonic Evolution of South America. In: Milani, Cordani, Thomaz-Filho, Campos (Eds.), . Río de Janeiro.

Cordani, U., Teixeira, W., D'Agrella-Filho, M.S., Trindade, R.I., 2009. The position of the Amazonia craton in supercontinents. Gondwana Research 15, 396–407.

Coutand, L., Chauvin, A., Cobbold, P.R., Gautier, P., Roperch, P., 1999. Vertical axis rotations across the Puna plateau northwestern Argentina and Chile. Journal of Geophysical Research 104, 22965–22984.

Da Silva, L.C., Gresse, P.G., Scheepers, R., McNaughton, N.J., Hartman, L.A., Fletcher, I., 2000. U–Pb SHRIMP and Sm–Nd age constraints on the timing and sources of the Pan-African Cape Granite Suite, South Africa. Journal of African Earth Sciences 30, 795–815.

Dalenz-Farjat, A., Álvarez, L.A., Hernández, R.M., Albariño, L.M., 2002. Cuenca Siluro-Devónica del Sur de Bolivia y del Noroeste Argentino: algunas interpretaciones. Congreso de Exploración y Desarrollo de Hidrocarburos, No. 5, CD-ROM Trabajos Técnicos. Mar del Plata.

Do Campo, M., Ribeiro Guevara, S., 2005. Provenance analysis and tectonic setting of late Neoproterozoic metasedimentary successions in NW Argentina. Journal of South American Earth Sciences 19, 143–153.

Drobe, M., López de Luchi, M., Steenken, A., Wemmer, K., Naumann, R., Frei, R., Siegesmund, S., 2009. Geodynamic evolution of the Eastern Sierras Pampeanas (Central Argentina) based on geochemical, Sm–Nd, Pb–Pb and SHRIMP data. International Journal of Earth Sciences. doi:10.1007/s00531-010-0593-3.

Enkin, R.J., 1994. A computer program package for analysis and presentation of paleomagnetic data. Pacific Geoscience Centre, Geological Survey of Canada. Sidney, Canada. 16 pp.

Enkin, R.J., 2003. The direction-correction tilt test: an all-purpose tilt/fold test for paleomagnetic studies. Earth and Planetary Science Letters 212, 151–166.

Escayola, M.P., Ramé, G.A., Kraemer, P.E., 1996. Caracterización y significado geotectónico de las fajas ultramáficas de Córdoba. 13° Congreso Geológico Argentino and 3° Congreso de Exploración de Hidrocarburos: Actas, 3, pp. 421–438.

Escayola, M.P., Pimentel, M.M., Armstrong, R., 2007. Neoproterozoic back-arc basin: sensitive high-resolution ion microprobe U–Pb and Sm–Nd isotopic evidence from the Eastern Pampean Ranges, Argentina. Geology 35, 495–498.

Evans, D.A.D., 1998. Supercontinental cycles and true polar wander. In: Bird, R.T., Powell, C., Wingate, McA (Eds.), The Assembly and Breakup of Rodinia; Proceedings of a Workshop. Abstracts. Geological Society of Australia, Sydney, NSW, Australia, pp. 34–35.

Fantini, R., Gromet, L.P., Simpson, C., Northrup, C.J., 1998. Timing of high-temperature metamorphism in the Sierras Pampeanas of Córdoba, Argentina: implications for Laurentia–Gondwana interactions. Actas X Congreso Latinoamericano de Geología and VI Congreso Nacional de Geología Económica, pp. 388–392.

Favetto, A., Pomposiello, C., López de Luchi, M.G., Booker, J., 2008. 2D Magnetotelluric interpretation of the crust electrical resistivity across the Pampean terrane–Río de la Plata suture, in central Argentina. Tectonophysics 459 (1–4), 54–65.

Fisher, R.A., 1953. Dispersion of a sphere. Proceeding of the Royal Society of London, Serie A 217, 295–305.

Forsythe, R.D., Davidson, I., Mpodozis, C., Jesinskey, C., 1993. Paleozoic relative motion of the Arequipa block and Gondwana: Paleomagnetic evidence from Sierra de Almeida of northern Chile. Tectonics 12, 219–236.

Gansser, A., 1973. Facts and theories on the Andes. Journal of the Geological Society 129, 93–131 London.

Germs, G.J.B., 1995. The Neoproterozoic of southwestern Africa, with emphasis on platform stratigraphy and paleontology. Precambrian Research 73, 137–151.

Geuna, S.E., Escosteguy, L.D., Miró, R., 2008. Palaeomagnetism of the Late Devonian–Early Carboniferous Achala Batholith, Córdoba, central Argentina: implications for the apparent polar wander path of Gondwana. Gondwana Research 13 (2), 227–237.

Gordon, R.G., 1991. Plate tectonic speed limits. Nature 349, 16–17.

Gromet, L.P., Simpson, C., 1999. Age of the Paso del Carmen pluton and implications for the duration of the Pampean Orogeny, Sierras de Córdoba. 14° Congreso Geológico Argentino: Actas, 1, pp. 149–151. Salta.

Grunow, A.M., 1995. Implications for Gondwana of new Ordovician paleomagnetic data from igneous rocks in southern Victoria Land, East Antarctica. Journal of Geophysical Research 100 (B7), 12589–12603.

Grunow, A.M., 1999. Gondwana events and paleogeography: a paleomagnetic review. Journal of African Earth Sciences 28 (1), 53–69.

Grunow, A.M., Encarnación, J.P., 2000. Cambro-Ordovician palaeomagnetic and geochronological data from southern Victoria Land, Antarctica: revision of the Gondwana apparent polar wander path. Geophysical Journal International 141, 391–400.

Gurnis, M., Torsvik, T.H., 1994. Rapid drift of large continents during the late Precambrian and Paleozoic: paleomagnetic constraints and dynamic models. Geology 22 (11), 1.023–1.026.

Hauser, N., Matteini, M., Omarini, R.H., Pimentel, M.M., 2011. Combined U -Pb and Lu -Hf isotope data on turbidites of the Paleozoic basement of NW Argentina and petrology of associated igneous rocks: Implications for the tectonic evolution of western Gondwana between 560 and 460 Ma. Gondwana Research 19 (1), 100–127.

Hernández, R.M., Reynolds, J., Disalvo, A., 1996. Análisis tectosedimentario y ubicación geocronológica del Grupo Orán en el río Iruya, Boletín de Informaciones Petroleras. Tercera Serie 12 (45), 80–93.

Hongn, F.D., Mon, R., 1999. Estructura del basamento pampeano en el noroeste de Argentina (provincias de Jujuy, Salta, Tucumán y Catamarca). In: González Bonorino, G., Omarini, R., Viramonte, J. (Eds.), Geología del Noroeste Argentino. Relatorio del 14° Congreso Geológico Argentino, pp. 80–88.

Hongn, F.D., Tubía, J.M., Aranguren, A., Vegas, N., Mon, R., Dunning, G.R., 2010. Magmatism coeval with lower Paleozoic shelf basins in NW-Argentina (Tastil batholith): constraints on current stratigraphic and tectonic interpretation. Journal of South Americn Earth Sciences 29, 289–305. doi:10.1016/j.jsames.2009.07.008.

Jacobs, J., Thomas, R.J., 2004. Himalayan-type indenter-escape tectonics model for the southern part of the late Neoproterozoic–early Paleozoic East African–Antarctic orogen. Geology 32, 721–724.

Jacobs, J., Bauer, W., Thomas, R.T., 2006. A Himalayan-type indentor-escape tectonic model for the southern part of the Late Neoproterozoic/Early Paleozoic East African/Antarctic Orogen. Geophysical Research Abstracts 8, 10297 2006. SRef-ID: 1607-7962/gra/EGU06-A-10297.

Jelinek, V., 1981. Characterization of the magnetic fabric of rocks. Tectonophysics 79, 63–67.

Keidel, J., 1943. El Ordovícico Inferior en los Andes del norte argentino y sus depósitos manino-glaciales. Boletín de la Academia Nacional de Ciencias, Córdoba. Tomo 36, 140–229.

Keppie, J.D., Bahlburg, H., 1999. Puncoviscana Formation of northwestern and Central Argentina: Passive margin or foreland basin deposits? In: Ramos, V.A., Keppie, J.D. (Eds.), Laurentia–Gondwana Connections before Pangea: Boulder, Colorado, Geological Society of American Special Paper, 336, pp. 139–143.

Kirschvink, J.L., 1980. The least-squares line and plane and the analysis of palaeomagnetic data. Geophysical Journal of the Royal Astronomical Society 62, 699–718.

Kleine, T., Mezger, K., Zimmermann, U., Munker, C., Bahlburg, H., 2004. Crustal evolution along the Early Ordovician proto-Andean margin of Gondwana: trace element and isotope evidence from the Complejo Igneo Pocitos (Northwest Argentina). Journal of Geology 112, 503–520.

Kley, J., 1996. Transition from basement-involved to thin-skinned thrusting in the Cordillera Oriental of southern Bolivia. Tectonics 15 (4), 763–775.

Konopásek, J., Kröner, S., Kitt, S.L., Passchier, C.W., Kröner, A., 2005. Oblique collision and evolution of large-scale transcurrent shear zones in the Kaoko belt, NW Namibia. Precambrian Research 136 (2), 139–157.

Kraemer, P.E., Escayola, M.P., Martino, R.D., 1995. Hipótesis sobre la evolución tectónica neoproterozoica de las Sierras Pampeanas de Córdoba (30° 40′–32° 40′), Argentina. Revista de la Asociación Geológica Argentina 50 (1–4), 47–59.

Krol, M.A., Simpson, C., 1999. 40Ar/39Ar Cooling ages from micas in the eastern Sierras Pampeanas accretionary prism rocks. Geological Society of America Abstract Programs 31, 114–115.

Kroner, A., Cordani, U., 2003. African, Southern Indian and South American craton were not part of the Rodinia supercontinent: evidence from field relations and geochronology. Tectonophysics 375, 325–352.

Loewy, S.L., Connelly, J.N., Dalziel, I.W.D., Gower, C.F., 2003. Eastern Laurentia in Rodinia: constraints from whole-rock Pb and U/Pb geochronology. Tectonophysics 375, 169–197.

Lucassen, F., Fowler, C.M.R., Franz, G., 1996. Formation of magmatic crust at the Andean continental margin during early Mesozoic: a geological and thermal model of the North Chilean Coast Range. Tectonophysics 262, 263–279.

Lucassen, F., Becchio, R., Wilke, M.F., Thirlwall, H.G., Viramonte, J., Franz, G., Wemmer, K., 2000. Proterozoic–Paleozoic development of the basement of the Central Andes (18°–26°) — a mobile belt of the South American craton. Journal of South American Earth Sciences 13, 697–715.

Maffione, M., Speranza, F., Faccenna, C., 2009. Bending of the Bolivian orocline and growth of the central Andean plateau: paleomagnetic and structural constraints from the eastern Cordillera (22–24°S, NW Argetina). Tectonics 28, TC4006. doi:10.1029/2008TC002402.

Mángano, M.G., Buatois, L.A., 2004. Integración de estratigrafía secuencial, sedimentología e icnología para un análisis cronoestratigráfico del Paleozoico inferior del noroeste argentino. Revista de la Asociación Geológica Argentina 59 (2), 273–280.

Martino, R., 2003. Las fajas de deformación dúctil de las Sierras Pampeanas de Córdoba: Una reseña general. Revista de la Asociación Geológica Argentina 58 (4), 549–571.

McElhinny, M.W., Powell, C. McA, Pisarevsky, S.A., 2003. Paleozoic terranes of eastern Australia and the drift history of Gondwana. Tectonophysics 362, 41–65.

McFadden, P.L., McElhinny, M.W., 1990. Classification of the reversal test in paleomagnetism. Geophysical Journal International 103, 725–729.

Meert, J.G., 2001. Growing Gondwana and rethinking Rodinia: a paleomagnetic perspective. Gondwana Research 4 (3), 279–288.

Meert, J.G., 2003. A synopsis of events related to the assembly of Eastern Gondwana. Tectonophysics 362, 1–40.

Meert, J.G., Torsvik, T.H., 2003. The making and unmaking of a supercontinent: Rodinia revisited. Tectonophysics 375, 261–288.

Meert, J.G., Van der Voo, R., 1996. Paleomagnetic and $^{40}Ar/^{39}Ar$ study of the Sinyai Dolerite, Kenya: implications for Gondwana Assembly. Journal of Geology 104, 131–142.

Meert, J.G., Nedelec, A., Hall, C., Wingate, M.T.D., Rakotondrazafy, M., 2001. Paleomagnetism, geochronology and tectonic implications of the Cambrian-age Carion granite, Central Madagascar. Tectonophysics 340, 1–21.

Meert, J.G., Nedelec, A., Hall, C., 2003. The stratoid granites of central Madagascar: paleomagnetism and further age constraints on Neoproterozoic deformation. Precambrian Research 120, 101–129.

Miró, R.C., Schwartz, J., Gromet, P., 2005. Magmatismo Calcoalcalino en la Sierra Norte de Córdoba. Su extensión temporal. In: Aceñolaza, F.G. (Ed.), Simposio Bodenbender, INSUGEO: Serie Correlación Geológica, 19, pp. 199–210.

Mon, R., Salfity, J.A., 1995. Tectonic evolution of the Andes of Northern Argentina. In: Tankard, A.J., Suaárez Soruco, R., Welsink, H.J. (Eds.), Petroleum basins of South America: AAPG Memoir, 62, pp. 269–283.

Mulcahy, S.R., Roeske, S.M., McClelland, W.C., Nomade, S., Renne, R., 2007. Cambrian initiation of the Las Pirquitas thrust of the western Sierras Pampeanas, Argentina: implications for the tectonic evolution of the proto-Andean margin of South America. Geology 35 (5), 443–446. doi:10.1130/G23436A.1.

Omarini, R.H., Sureda, R.J., 1994. El basamento centroandino y sus cuencas marginales entre el rift Iruyico (515 Ma y la colision ocloyica (435 Ma)). 7° Congreso Geológico Chileno, Concepción, pp. 491–497.

Pavlov, V., Gallet, Y., 1998. Upper Cambrian to Middle Ordovician magnetostratigraphy from the Kulumbe River section (Northwestern Siberia). Physics of the Earth and Planetary Interiors 108, 49–59.

Piñán Llamas, A., Simpson, C., 2006. Deformation of Gondwana margin turbidites during the Pampean orogeny, north-central Argentina. Geological Society of America Bulletin 118 (9/10), 1270–1279.

Porada, H., Berhorst, V., 2000. Towards a new understanding of the Neoproterozoic–Early Palaeozoic Lufilian and northern Zambezi Belts in Zambia and the Democratic Republic of Congo. Journal of African Earth Sciences 30, 727–771.

Preciozzi, F., Basei, M.A., Masquelín, H., 1999. New geochronological data from the Piedra Alta Terrane (Río de la Plata Craton). II Simposio Sudamericano de Geología Isotópica : 341–344. Villa Carlos Paz. Córdoba. Argentina.

Prezzi, C., Caffe, P., Somoza, R., 2004. New paleomagnetic data from the northern Puna and western Cordillera Oriental, Argentina: a new insight on the timing of rotational deformation. Journal of Geodynamics 38 (2), 93–115.

Ramé, G.A., Miró, R., 2010. Estudio gravimétrico del borde occidental del cratón del Río de la Plata. 6° Congreso Uruguayo de Geología. Abstracts in CD.

Ramos, V.A., 1988. Tectonics of the Late proterozoic–Early Paleozoic: a collisional history of southern South America. Episodes 11 (3), 168–174.

Ramos, V.A., 1999. Las Provincias geológicas del territorio argentino. Instituto de Geología y Recursos Minerales. Geología Argentina. Anales 29 (24), 41–96.

Ramos, V.A., 2000. The southern Central Andes. In: Cordani, U.G., Milani, E.J., Thomaz Filho, A., Campos, D.A. (Eds.), Tectonic Evolution of South America: 31° International Geological Congress, Río de Janeiro, pp. 561–604.

Ramos, V.A., 2004. Cuyania, an exotic block to Gondwana: review of a historical success and the present problems. Gondwana Research 7, 1009–1026.

Ramos, V.A., 2008. The basement of the Central Andes: the Arequipa and related terranes. Annual Review of Earth and Planetary Sciences 36, 289–324.

Ramos, V.A., Vujovich, G., Martino, R., Otamendi, J., 2010. Pampia: a large cratonic block missing in the Rodinia supercontinent. Journal of Geodynamics 50 (3–4), 243–255.

Randall, E., 1998. A Jurassic–Recent apparent polar wander path for South America and review of central Andean tectonic models. Tectonophysics 299, 49–74.

Rapalini, A.E., 2005. The accretionary history of Southern South America from the latest Proterozoic to the Late Paleozoic: some paleomagnetic constraints. In: Vaughan, A., Leat, P., Pankhurst, R.J. (Eds.), Terrane Processes at the Margins of Gondwana: Geological Society of London, Special Publication, 246, pp. 305–328.

Rapalini, A.E., Astini, R.A., Conti, C.M., 1999. Paleomagnetic constrains on the evolution of Paleozoic suspect terranes from southern South America. In: Ramos, V.A., Keppie, J.D. (Eds.), Laurentia–Gondwana Connections before Pangea. Boulder, Colorado: Geological Society of American Special Paper, 336, pp. 171–184.

Rapalini, A.E., Velasco, M.S., Koukharsky, M., 2002. New paleomagnetic data from the Western Puna of Argentina: some tectonic speculations on its Early Paleozoic evolution. 5th International Symposium on Andean Geodynamics, pp. 505–508. Extended Abstracts.

Rapela, C.W., 2000. Discusión: El ambiente geotectónico del Ordovícico de la región del Famatina: Comentario. Revista de la Asociación Geológica Argentina 55 (1–2), 134–136.

Rapela, C.W., Pankhurst, R.J., Casquet, C., Baldo, E., Saavedra, J., Galindo, C., 1998a. Early evolution of the proto-Andean margin of South America. Geology 26 (8), 707–710.

Rapela, C.W., Pankhurst, R.J., Casquet, C., Baldo, E., Saavedra, J., Galindo, C., Fanning, C.M., 1998b. The Pampean orogeny of the southern proto-Andes: Cambrian continental collision in the Sierras de Córdoba. In: Pankhurst, R.J., Rapela, C.W. (Eds.), The Proto-Andean Margin of Gondwana: Geological Society, London, Special Publications, 142, pp. 181–217.

Rapela, C.W., Casquet, C., Baldo, E., Dahlquist, J., Pankhurst, R.J., Galindo, C., Saavedra, J., 2001. Las Orogénesis del Paleozoico Inferior en el margen proto-andino de América del Sur, Sierras Pampeanas, Argentina. Journal of Iberian Geology 27, 23–41.

Rapela, C.W., Pankhurst, R.J., Casquet, C., Fanning, C.M., Baldo, E.G., González-Casado, J.M., Galindo, C., Dahlquist, J., 2007. The Río de la Plata craton and the assembly of SW Gondwana. Earth Science Reviews 83, 49–82.

Reeves, C.V., de Wit, M.J., Sahu, B.K., 2004. Tight reassembly of Gondwana exposes Phanerozoic shears in Africa as global tectonic players. Gondwana Research 7, 7–19.

Reynolds, J.H., Hernández, R., Galli, C., Idelman, B., 2001. Magnetostratigraphy of the Quebrada La Porcelana section, Sierra de Ramos, Salta province, Argentina. Initial age limits on the regional Neogene lithostratigraphy and uplift of the southern Sierras Subandinas. Journal or South American Earth Sciences 14, 681–692.

Ring, U., Kroner, A., Buchwaldt, R., Toulkeridis, T., Layer, P.W., 2002. Shear-zone patterns and eclogite-facies metamorphism in the Mozambique belt of northern Malawi, east-central Africa: implications for the assembly of Gondwana. Precambrian Research 116, 19–56.

Rozendaal, P.G., Gresse, R., Scheeps, J.P., Roux, Le, 1999. Neoproterozoic to Early Cambrian crustal evolution of the Pan-African Saldania Belt. South Africa, Precambrian Research 97, 303–323.

Sánchez Bettucci, L., Rapalini, A.E., 2002. Paleomagnetism of the Sierras de las Ánimas Complex, Southern Uruguay: its implications in the assembly of western Gondwana. Precambrian Research 118, 243–265.

Sánchez, M.C., Salfity, J.A., 1999. La cuenca cámbrica del Grupo Mesón en el Noroeste Argentino: desarrollo estratigráfico y paleogeográfico. Acta Geologica Hispánica 34 (2–3), 123–139.

Schwartz, J.J., Gromet, L.P., 2004. Provenance of a late Proterozoic–early Cambrian basin, Sierras de Córdoba, Argentina. Precambrian Research 129, 1–21.

Schwartz, J.J., Gromet, L.P., Miro, R., 2008. Timing and duration of the calc-alkaline arc of the Pampean Orogeny: implications for the Late Neoproterozoic to Cambrian evolution of Western Gondwana. Journal of Geology 116, 39–61.

Simpson, C., Lan, R.D., Gromet, L.P., Miro, R., Northrup, C.J., 2003. Paleozoic deformation in the Sierras de Córdoba and Sierra de las Minas, eastern Sierras Pampeanas, Argentina. Journal of South American Earth Sciences 15, 749–764.

Sims, J.P., Ireland, T.R., Camacho, A., Lyons, P., Pieters, P.E., Skirrow, R.G., Stuartsmith, P.G., 1998. U–Pb, Th–Pb and Ar–Ar geochronology from the southern Sierras Pampeanas, Argentina: implications for the Palaeozoic tectonic evolution of the western Gondwana margin. In: Pankhurst, R.J., Rapela, C.W. (Eds.), The Proto-Andean Margin of Gondwana: Geological Society (London) Special Publication, 142, pp. 259–281.

Somoza, R., Singer, S., Coira, B., 1996. Paleomagnetism of upper miocene ignimbrites at the Puna: an analysis of vertical-axis rotations in the Central Andes. Journal of Geophysical Research 101, 11387–11400.

Spagnuolo, C.M., Rapalini, A.E., Astini, R.A., 2005. Preliminary paleomagnetic results from the Cambrian Mesón group: implications for the Bolivian Orocline. 6° International Symposium of Andean Geodynamics, Barcelona, España.

Spagnuolo, C.M., Rapalini, A.E., Astini, R.A., 2008. Paleogeographic and tectonic implications of the first paleomagnetic results from the Middle–Late Cambrian Meson Group: NW Argentina. Journal of South American Earth Sciences 25, 86–99.

Steenken, A., Wemmer, K., López de Luchi, M.G., Siegesmund, S., Pawlig, S., 2004. Crustal provenace and cooling of the basement complexes of the Sierra de San Luis: an insight into the tectonic history of the proto-Andean margin of Gondwana. Gondwana Research 7 (4), 1171–1195.

Tohver, E., D'Agrella-Filho, M.S., Trindade, R.I.F., 2006. Paleomagnetic record oa Africa and South America for the 1200–500 Ma interval, and evaluation of Rodinia and Gondwana assemblies. Precambrian Research 147, 193–222.

Tohver, E., Cawood, P., Rossello, E., Lopez de Luchi, M.G., Rapalini, A., Jourdan, F., 2008. New SHRIMP U–Pb and $^{40}Ar/^{39}Ar$ constraints on the crustal stabilization of southern South America, from the margin of the Rio de Plata (Sierra de Ventana) craton to northern Patagonia. Eos Trans. AGU, 89 (53). Fall Meeting, Abstract, T23C-2052.

Tohver, E., Trindade, R.I.F., Solum, J.G., Hall, C.M., Riccomini, C., Nogueira, A.C., 2010. Closing the Clymene ocean and bending a Brasiliano belt: evidence for the Cambrian formation of Gondwana, southeast Amazon craton. Geology 38, 267–270. doi:10.1130/G30510.1.

Torsvik, T.H., Briden, J.C., y Smethurst, M.A., 2000. IAPD2000 (Interactive Analysis of Palaeomagnetic Data). Norwegian Geophysical Union.

Tosdal, R.M., 1996. The Amazon–Laurentian connection as viewed from Middle Proterozoic rocks in the central Andes, western Bolivia and northern Chile. Tectonics 15, 827–842.

Trindade, R.I.F., D'Agrella-Filho, M.S., Babinsky, M., Font, E., Brito Neves, B.B., 2004. Paleomagntism and geochronology of the Bebedoura cap carbonate: evidence for continental-scale Cambrian remagnetization in te Sao Francisco craton, Brazil. Precambrian Research 128 (1–2), 83–103.

Trindade, R.I.F., D'Agrella-Filho, M.S., Epof, I., Brito Neves, B.B., 2006. Paleomagnetism of Early Cambrian Itabaiana mafic dikes (NE Brazil) and the final assembly of Gondwana. Earth and Planetary Science Letters 244, 361–377.

Trompette, R., De Alvarenga, C.J.S., Walde, D., 1998. Geological evolution of the Neoproterozoic Corumba graben system (Brazil). Depositional context of the stratified Fe and Mn ores of the Jacadigo group. Journal of South American Earth Sciences 11 (6), 587–597.

Turner, J.C.M., 1960. Estratigrafía de la Sierra de Santa Victoria y adyacencias. Boletín de la Academia Nacional de Ciencias de la República Argentina 41 (2), 163–196.

Turner, J.C.M., Méndez, V., 1975. Geología del sector oriental de los Departamentos de Santa Victoria e Iruya, Provincia de Salta, República Argentina. Boletín de la Academia Nacional de Ciencias de Córdoba 51 (1–2), 11–24.

Van der Voo, R., 1990. The reliability of paleomagnetic data. Tectonophysics 184, 1–9.

Vaughan, A.P.M., Pankhurst, R.J., 2008. Tectonic overview of the West Gondwana margin. Gondwana Research 13, 150–162.

Villar, L.M., 1975. Las fajas y otras manifestaciones ultrabásicas en la República Argentina y su significado metalogenético. 2° Congreso Ibero-Americano de Geología Económica: Actas, 3, pp. 135–155. Buenos Aires.

von Gosen, W., Loske, W., Prozzi, C., 2002. New isotopic dating of intrusive rocks in the Sierra de San Luis (Argentina): implications for the geodynamic history of the Eastern Sierras Pampeanas. Journal of South American Earth Sciences 15, 237–250.

Watson, G., Enkin, R., 1993. The fold test in paleomagnetism as a parameter estimation problem. Geophysical Research Letters 20 (19), 2135–2137.

Whitmeyer, S.J., Simpson, C., 2003. High strain-rate deformation fabrics characterize a kilometer-thick Paleozoic fault zone in the Eastern Sierras Pampeanas, central Argentina. Journal of Structural Geology 25, 909–922.